

Review

# Graphene in Polymeric Nanocomposite Membranes—Current State and Progress

Ayesha Kausar <sup>1,2,3,\*</sup> , Ishaq Ahmad <sup>1,2,3</sup>, Tingkai Zhao <sup>1,4</sup>, O. Aldaghri <sup>5</sup>  and M. H. Eisa <sup>5</sup>

<sup>1</sup> NPU-NCP Joint International Research Center on Advanced Nanomaterials and Defects Engineering, Northwestern Polytechnical University, Xi'an 710072, China

<sup>2</sup> UNESCO-UNISA Africa Chair in Nanosciences/Nanotechnology, iThemba LABS, Somerset West 7129, South Africa

<sup>3</sup> NPU-NCP Joint International Research Center on Advanced Nanomaterials and Defects Engineering, National Centre for Physics, Islamabad 44000, Pakistan

<sup>4</sup> School of Materials Science & Engineering, Northwestern Polytechnical University, Xi'an 710072, China

<sup>5</sup> Department of Physics, College of Science, Imam Mohammad Ibn Saud Islamic University (IMSIU), Riyadh 13318, Saudi Arabia

\* Correspondence: dr.ayeshakausar@yahoo.com

**Abstract:** One important application of polymer/graphene nanocomposites is in membrane technology. In this context, promising polymer/graphene nanocomposites have been developed and applied in the production of high-performance membranes. This review basically highlights the designs, properties, and use of polymer/graphene nanocomposite membranes in the field of gas separation and purification. Various polymer matrices (polysulfone, poly(dimethylsiloxane), poly(methyl methacrylate), polyimide, etc.), have been reinforced with graphene to develop nanocomposite membranes. Various facile strategies, such as solution casting, phase separation, infiltration, self-assembly, etc., have been employed in the design of gas separation polymer/graphene nanocomposite membranes. The inclusion of graphene in polymeric membranes affects their morphology, physical properties, gas permeability, selectivity, and separation processes. Furthermore, the final membrane properties are affected by the nanofiller content, modification, dispersion, and processing conditions. Moreover, the development of polymer/graphene nanofibrous membranes has introduced novelty in the field of gas separation membranes. These high-performance membranes have the potential to overcome challenges arising from gas separation conditions. Hence, this overview provides up-to-date coverage of advances in polymer/graphene nanocomposite membranes, especially for gas separation applications. The separation processes of polymer/graphene nanocomposite membranes (in parting gases) are dependent upon variations in the structural design and processing techniques used. Current challenges and future opportunities related to polymer/graphene nanocomposite membranes are also discussed.

**Keywords:** membrane; graphene; polymer; nanocomposite; high performance; gas separation



**Citation:** Kausar, A.; Ahmad, I.; Zhao, T.; Aldaghri, O.; Eisa, M.H. Graphene in Polymeric Nanocomposite Membranes—Current State and Progress. *Processes* **2023**, *11*, 927. <https://doi.org/10.3390/pr11030927>

Academic Editors: Mohammad Boshir Ahmed, Md Ashraf Hossain, Mohammad Shamsuddin Ahmed and Jivan Thakare

Received: 18 February 2023

Revised: 8 March 2023

Accepted: 13 March 2023

Published: 18 March 2023



**Copyright:** © 2023 by the authors. Licensee MDPI, Basel, Switzerland. This article is an open access article distributed under the terms and conditions of the Creative Commons Attribution (CC BY) license (<https://creativecommons.org/licenses/by/4.0/>).

## 1. Introduction

Membrane technology has been applied to achieve the selective separation of noxious or desired gas molecules [1,2]. Polymeric membranes have gained significance for gas separation purposes [3]. Graphene is a unique type of nanocarbon nanostructure that can be oxidized to form graphene oxide [4]. Pristine porous graphene nanosheets demonstrate high selectivity and permeability for the purposes of gas separation [5]. Similar to other nanocarbons (carbon nanotube, fullerene, nanodiamond, etc.), graphene and graphene oxide can function as effective nano-reinforcements for polymeric membranes [6]. Consequently, polymer/graphene nanocomposite membranes have been used for the efficient separation of gas molecules [7–9]. High-performance gas separation membranes have been developed using facile processing techniques [10]. Polymer/graphene-based gas separation

membranes with nanoporous, ultrathin, and mixed-matrix properties have mainly been fabricated using solution routes, infiltration, phase inversion techniques, and other facile strategies [11–13]. Polymer/graphene membranes have been developed using polysulfone, polyimide, poly(methyl methacrylate), poly(dimethyl siloxane), polyamide, and other polymeric matrices. The high selectivity and molecular diffusivity of gas separation membranes are affected by their pore size, pore distribution, graphene dispersion, and fabrication route. Homogeneous graphene dispersions produce tortuous pathways for the selective diffusion of gaseous molecules [14]. Due to their ability to efficiently separate gaseous pollutants, gas separation membranes have been applied in chemical industries [15]. Moreover, gas separation membranes have also found significant application in fuel cells, gas sensors, and in other technical fields [16].

To achieve the efficient fabrication of graphene-based gas separation membranes, the mechanisms of gas transport through these membranes need to be thoroughly understood. Supported, self-standing, and nanocomposite membrane materials need to be studied in light of new design innovations [17]. In addition to graphene, graphene derivatives such as graphene oxide, reduced graphene oxide, etc., could broaden the application potential of these membranes. Gas molecules can pass through defects in nanosheets or through the interlayer spacing between graphene oxide or modified graphene nanosheets. Graphene oxide-based membranes offer high values of flux due to their ultimate thinness [18]. Moreover, graphene oxide offers high selectivity through molecular sieving or diffusion as a result of its narrow pore size distribution and unique surface chemistry. The interlayer spacing between graphene nanosheets can be tailored to achieve optimal transportation of the desired molecules through the membrane [19]. Graphene derivatives could potentially be used to overcome the limitations whereby permeability must be sacrificed to obtain better selectivity [20]. In particular, the interlayer spacing between graphene derivative layers could be controlled in order to selectively separate out the desired gases from a gas mixture. The selection of appropriate graphene derivative-based support materials could be a research focus for the development of high-performance nanocomposite membranes [21]. Such support materials may allow the membranes to tolerate challenging process conditions such as high temperature, high pressure, corrosive environment, humidity, etc. [22]. Consequently, such membranes are able to achieve high selectivity and high flux. These efforts could facilitate the development of high-performance graphene-based membranes that are able to fill the gaps between basic membrane designs, large-scale production, and commercialization.

This review fundamentally focuses on the design, fabrication, and properties of polymer/graphene nanocomposite membranes with respect to gas permeability and selectivity. The use of graphene nanofillers has widened the scope of gas permeation membranes. This review systematically presents the advancements in the field of polymer/graphene nanocomposite membranes for the purposes of gas separation. Polymer/graphene nanocomposite membranes demonstrate the ability to overcome the challenges presented by gaseous mixture environments in the separation of desired gases/contaminants. To the best of our knowledge, such a specific and up-to-date review of polymer/graphene nanocomposite gas separation membranes has not previously been seen in the literature. There have been significant recent literature reports (i.e., between 2018 and 2023) on the polymer/graphene nanocomposite membranes for the purposes of gas separation, as discussed in this article. Thus, this state-of-the-art review highlights the novelties of high-performance gas separation polymer/graphene nanocomposite membranes. Moreover, future attempts by scientists/researchers to achieve progress in the field of polymer/graphene nanocomposite membranes will not be possible without prior knowledge of the reported literature compiled here.

## 2. Polymer Nanocomposite-Based Membranes

Various polymeric materials and design strategies have been used for the development of advanced membranes [23]. Numerous nanofillers (carbon nanoparticles, metal oxide,

metal nanoparticle) have been reinforced in matrices to form the polymeric nanocomposite membranes [24–26]. Incorporation of nanoparticles in polymers enhanced the mechanical, thermal, and durability properties of the membranes [27–29]. Moreover, nanoparticles affect the membranes morphology to develop a nanoporous structure for gas separation [30–32]. The membrane properties and performance depend on the nanofiller type, contents, and reinforcement conditions [33]. Consequently, the polymer/inorganic nanoparticle nanocomposite membranes have been designed for gas separation having fine selectivity, permeability, and superior physical properties [34]. In this context, interactions between polymer-nanofiller and separation mechanisms of the nanocomposite membranes have been investigated [35,36].

Among inorganic nanoparticles, silica nanoparticles have been reinforced in the nanocomposite membranes [37–39]. Matavos-Aramyan et al. [40] produced the polyurethane/silica and polyesterurethane/silica nanocomposite membranes. The membranes were fabricated using the solvent casting and solvent evaporation methods. The membranes were tested for the permeation of CO<sub>2</sub>, O<sub>2</sub>, and N<sub>2</sub> gases. The nanocomposite membranes revealed efficient CO<sub>2</sub>/N<sub>2</sub> and O<sub>2</sub>/N<sub>2</sub> separation performance [41]. Khedary et al. [42] designed the poly(vinylidene-fluoride-hexafluoropropylene)/amino-silica nanoparticle-based nanocomposite membranes. Phase separation method was adopted for the membrane fabrication. The surface area of the poly(vinylidene-fluoride-hexafluoropropylene)/amino-silica nanocomposite was higher (116.4 m<sup>2</sup>/g), as compared with the pristine polymer (3.8 m<sup>2</sup>/g). Figure 1 shows the poly(vinylidene-fluoride-hexafluoropropylene) membranes with well dispersed amino-silica nanoparticles. Adding 40 wt.% nanofiller content revealed high CO<sub>2</sub> uptake of 33.75 mg/g. Consequently, the nanoporous membranes were efficient for CO<sub>2</sub> separation. Adding silica nanoparticles formed phase separated structure that is suitable for parting or capturing the CO<sub>2</sub> molecules. Gas separation properties were dependent on the diffusion-sorption mechanism. Consequently, polymer/silica nanocomposite membranes have high gas permeability characteristics due to fine nanofiller dispersion and matrix-nanofiller compatibility [43]. Gas selectivity and permeability depend upon the nanofiller dispersal properties, thus leading to the development of gas diffusion pathways [44]. In this regard, modification of polymeric backbone could enhance the membrane flexibility, durability, and permeation properties [45]. Moreover, large-scale production of these membranes has been a focus for commercial applications [46].

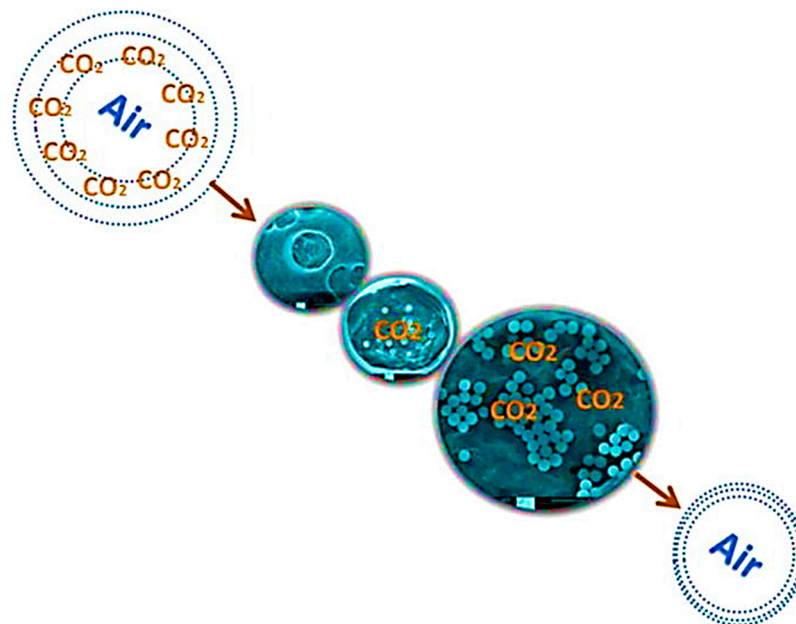


**Figure 1.** Schematic of CO<sub>2</sub> separation by poly(vinylidene-fluoride-hexafluoropropylene)/amino-silica nanoparticle based nanocomposite membranes [42]. Reproduced with permission from Elsevier.

In addition to silica, titania nanoparticles have also been used as the polymeric membrane reinforcements [47]. The polymer/TiO<sub>2</sub> membranes revealed fine structural stability and physical characteristics for gas or water purification [48]. Furthermore, zinc oxide nanoparticles have been filled in the polymeric membranes for gas separation [49]. The cellulose acetate/zinc oxide nanocomposite membranes with 0.7 wt.% nanofiller contents revealed CO<sub>2</sub>/H<sub>2</sub> selectivity of 2.77. Besides, the nanocarbon nanoparticles such as carbon nanotube [50–52], fullerene [53–55], and nanodiamond [56–58] have been reinforced in the polymeric membranes for gas separation. The polymeric nanocomposite membranes have found applications in water treatment [59], gas separation [60], and fuel cells [61].

### 3. Graphene

Graphene is a two-dimensional (one atom thick) nanosheet made up of sp<sup>2</sup> hybridized carbon atoms [62]. Graphene was discovered in 2004 [63]. Various facile synthesis routes have been used for developing single-layer graphene such as graphite exfoliation, mechanical cleavage, chemical vapor deposition, plasma method, and organic synthesis approaches [64–66]. Graphene has been identified as a thin and transparent nanocarbon nanostructure [67]. Young's modulus of a single graphene nanosheet was significantly high, i.e., ~1 TPa, so it is >200 times stronger than steel [68]. High thermal conductivity was observed in the range of 3000–5000 W/mK [69]. Moreover, it has high electron mobility of 200,000 cm<sup>2</sup>·V<sup>-1</sup>·s<sup>-1</sup>. Graphene has a wrinkling tendency due to van der Waals forces [70]. Therefore, graphene has been functionalized to form graphene oxide nanosheet having hydrophilic groups (hydroxyl, carboxylic, epoxide, and carbonyl) on the surface. An important use of graphene has been observed in the nanocomposites [71]. The graphene-based nanocomposites revealed remarkable mechanical stability, electrical conductivity, thermal conductivity, thermal stability, chemical stability, and other physical properties. Applications of the graphene-derived nanocomposites have been observed in membranes [72], coatings [73], energy devices [74], fuel cell [75], sensors [76], batteries [77], and tissue engineering/drug delivery [78].

Graphene is no doubt the mother of graphitic forms of carbon with sp<sup>2</sup> hybridized carbon atoms in a honeycomb hexagonal arrangement [79]. Graphene has several derived forms such as graphene oxide and reduced graphene oxide [80]. Graphene oxide is a derivative of graphene that is formed by an oxidation-exfoliation process. Graphene oxide is a two-dimensional crystalline structure with a hexagonal pattern and functional oxygen groups on the surface [81]. Graphene oxide has sp<sup>2</sup> hybridization, π–π interactions, and versatile conjugation with other molecules [82]. Due to oxygen functional groups on the surface, graphene oxide has the ease of dissolution in water and other solvents [83]. Graphene oxide has facile large-scale production and commercialization. Figure 2 shows a graphene nanosheet, graphene oxide, and reduced graphene oxide nanostructures [84]. Graphene oxide is obtained by the oxidation of graphite, while reduced graphene oxide can be synthesized by the reduction of graphene oxide. The reduced graphene oxide has layered nanosheets without any oxygenated groups on the surface. In this regard, chemical and electrochemical reduction routes have been used to reduce the surface carboxylic acid and oxygen functional groups [85]. Graphene quantum dot is also an interesting form of graphene. Its size is less than 10 nm. The graphene quantum dot has fine optical absorption and electroluminescence properties [86]. Graphene derivatives have been applied in membrane technology.



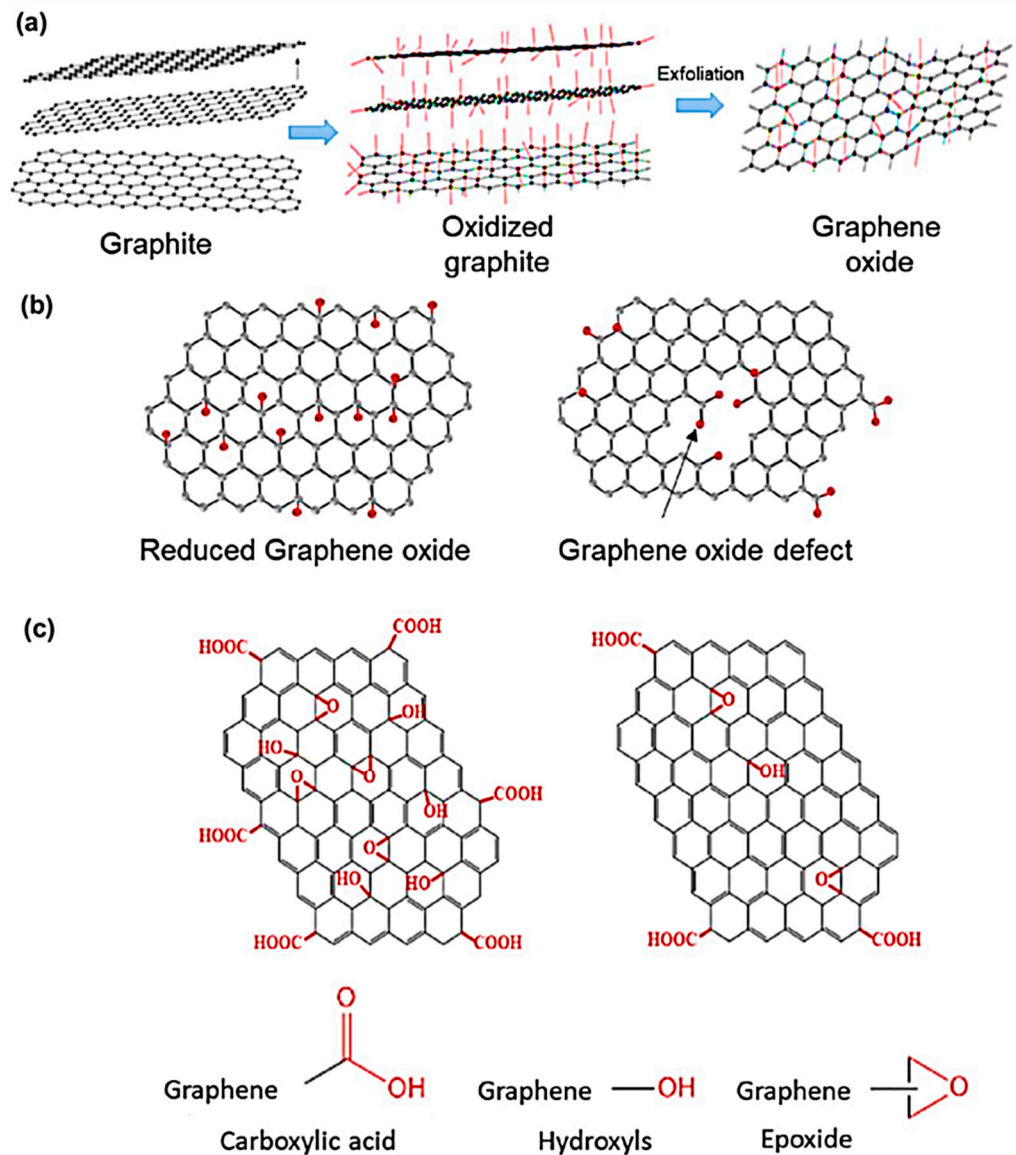


**Figure 2.** (a) Graphene oxide obtained by graphite exfoliation; (b) is presented in the reduced graphene oxide structured, as the graphene oxide defect. (c) Reactive groups present in graphene oxide and reduced graphene oxide [87]. Reproduced with permission from Springer.

#### 4. Gas Separation Membranes Derived from Polymer/Graphene Nanocomposites

Graphene has been used to develop the nanoporous membranes for gas molecules transportation [88,89]. Lee et al. [90] fabricated the graphene-based membrane to separate  $\text{CO}_2$  from the mixture of gases ( $\text{CO}_2/\text{O}_2$ ,  $\text{CO}_2/\text{N}_2$ , and  $\text{CO}_2/\text{CH}_4$ ). Figure 3 depicts interaction between  $\text{CO}_2$  molecules and graphene nanosheets. The size of graphene pores facilitated the passage of  $\text{CO}_2$  molecules. Moreover, graphene was found to have greater affinity towards the  $\text{CO}_2$  molecules [91]. Flux and selectivity of  $\text{CO}_2/\text{O}_2$ ,  $\text{CO}_2/\text{N}_2$ , and  $\text{CO}_2/\text{CH}_4$  are given in Table 1. Higher  $\text{CO}_2/\text{O}_2$  flux (0.43) was observed due to an optimum diameter of the gas molecules, compared with other gas mixtures [92]. Selectivity of  $\text{CO}_2/\text{O}_2$  was also found to be optimum. Consequently, the pristine graphene nanosheet was successfully used for thin high performance gas separation membranes [93].

Koenig et al. [94] developed the graphene membranes on silicon oxide substrate. The small  $\text{H}_2$  molecules were easily separated through the nanoporous membrane. However, after etching, large size molecules were also allowed to pass through the membrane and small  $\text{H}_2$  molecules were leaked out of the chamber (Figure 4). Figure 5 compares the leak

rates ( $-d\delta/dt$ ) of the pristine graphene membrane and the etched membrane. The  $-d\delta/dt$  for gases depends on the molecular sizes of the gas molecules. The results suggested that the etched membrane affected the transport mechanism of H<sub>2</sub> and CO<sub>2</sub> gases due to bulging and membrane distortion.

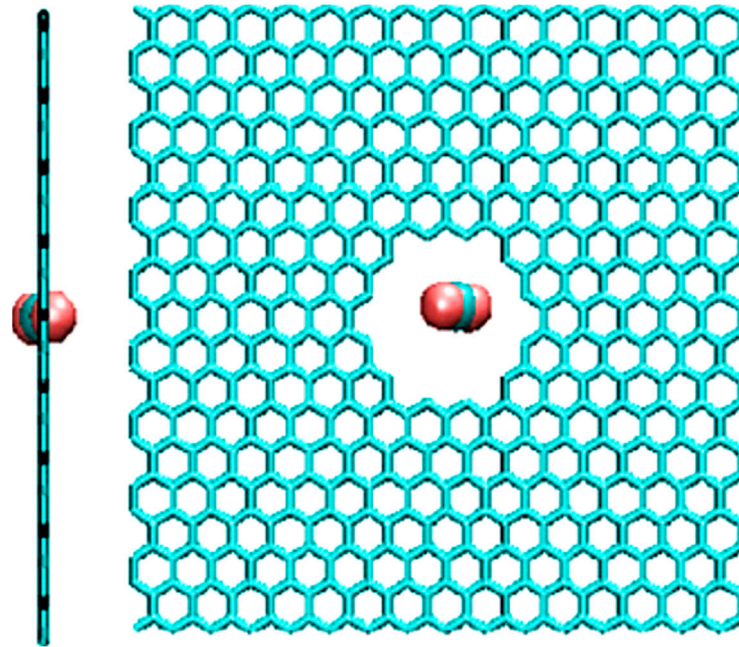


**Figure 3.** Configuration of CO<sub>2</sub> molecule in graphene pore [90]. Reproduced with permission from Elsevier.

**Table 1.** Separation of CO<sub>2</sub> from different gas mixtures using graphene membrane [90]. Reproduced with permission from Elsevier.

| Gas Mixture or Gas               | CO <sub>2</sub> Flux (No. of Molecules) | Selectivity | Size of Gas Molecules Kinetic Diameter (pm) |
|----------------------------------|---|-------------|---|
| CO <sub>2</sub> /O <sub>2</sub>  | 0.43 ± 0.04                             | 9.5 ± 0.7   | -   |
| CO <sub>2</sub> /N <sub>2</sub>  | 0.23 ± 0.06                             | 14.4 ± 1.4  | -   |
| CO <sub>2</sub> /CH <sub>4</sub> | 0.35 ± 0.12                             | 9.9 ± 0.7   | -   |
| H <sub>2</sub>                   | -                                       | -           | 289   |
| CO <sub>2</sub>                  | -                                       | -           | 330   |
| O <sub>2</sub>                   | -                                       | -           | 346   |
| N <sub>2</sub>                   | -                                       | -           | 364   |
| CH <sub>4</sub>                  | -                                       | -           | 384   |

The nanoporous gas separation polymer/graphene membranes have been fabricated [95]. Li et al. [96] formed the polymer/graphene nanocomposite membranes having a pore size of 1 nm. The nanocomposite membranes revealed high selectivity for H<sub>2</sub>/N<sub>2</sub> (900) and H<sub>2</sub>/CO<sub>2</sub> (3400). The graphene-based nanocomposite membranes have been developed with a pore size of ~0.34 nm [97,98]. In addition to graphene, graphene oxide has also been used to form nano-galleries in the membranes for the molecular sieving of CO<sub>2</sub> and other molecules [99]. Polysulfone membranes have been developed for gas separation [100–102]. The polysulfone matrix was used to form the symmetric mixed-matrix membranes [103]. These membranes have been applied for separating CO<sub>2</sub> and other noxious gases from the gas mixture [104]. Zahri et al. [105] fabricated the polysulfone/graphene oxide nanocomposite membranes. Graphene oxide was embedded in the polysulfone matrix forming a hollow fiber mixed matrix membrane. Dimethyl acetamide solvent was used for the dispersion of polymer and nanofiller. Spinning and dry-wet phase inversion techniques were applied for fabricating the asymmetric hollow fiber membranes. Figure 6 shows

the scanning electron microscopy cross section images of pristine polysulfone and polysulfone/graphene oxide-based mixed matrix membrane, including 0.25 wt.% graphene oxide-produced multi-layered structure with dense skin layer, porous sponge-like sub-layer, and large macro-void structure. However, the layered morphology was not found in a neat polymer membrane. Incorporating nanofiller in polysulfone enhanced the CO<sub>2</sub>/CH<sub>4</sub> separation from 19 to 25. The CO<sub>2</sub> permeance was also increased from 64.47 to 86.80 GPU. Effect was observed due to better interactions of CO<sub>2</sub> gas molecules with the graphene oxide nanofiller in the polymer matrix. Moreover, the graphene dispersion limited the permeation of large gas molecules, while allowing the passage of small molecules. In another attempt [106], the selectivity of CO<sub>2</sub>/N<sub>2</sub> and CO<sub>2</sub>/CH<sub>4</sub> was increased by 158% and 74%, respectively, for polysulfone/graphene nanocomposite, compared with the neat polysulfone membrane.

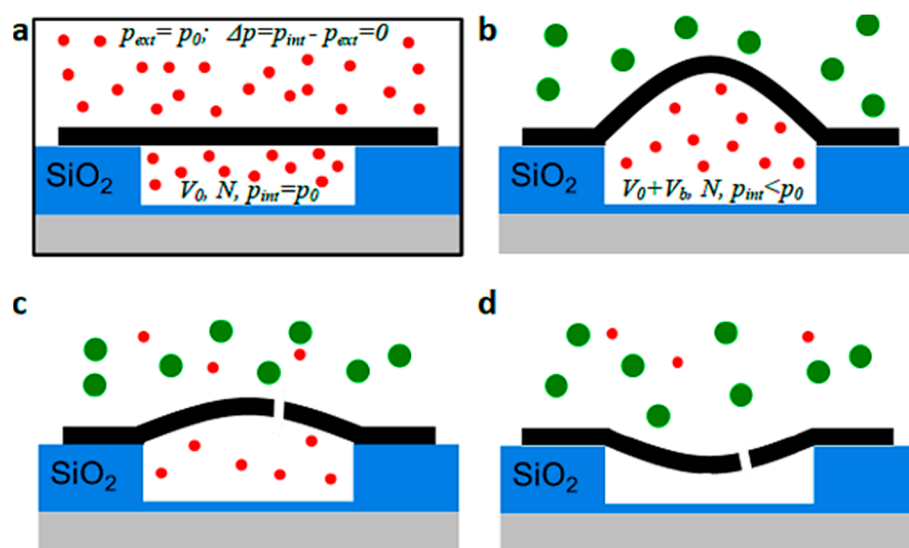


**Figure 4.** Measuring leak rates in porous graphene membranes: (a) schematic of microscopic graphene membrane on silicon oxide substrate; (b) after removing graphene membrane from pressure chamber, the membrane is bulged upward; (c) upon etching of graphene membrane, pore(s) bigger than that of H<sub>2</sub> are introduced allowing H<sub>2</sub> to leak rapidly out of microchamber through graphene membrane; and (d) after all H<sub>2</sub> molecules have leaked out of microchamber, the membrane will be bulged downward [94]. Red spheres = small H<sub>2</sub> molecules; green spheres = larger CO<sub>2</sub> gas molecules. Reproduced with permission from Nature.

Sainath et al. [107] developed the polysulfone/graphene oxide nanocomposite-based hollow fiber mixed matrix membrane for gas separation. In solution route, the polymer and 0.25 wt.% graphene oxide were dispersed in the N-Methyl-2-pyrrolidone solvent. The membrane has CO<sub>2</sub>/CH<sub>4</sub> selectivity of 45, i.e., 3.3 times higher than the selectivity of neat polymer membrane. Membrane properties were observed due to better graphene dispersion and diffusion path formation in the nanocomposite membranes. Zhu et al. [108] fabricated the polyphenylsulfone-pyridine/graphene oxide nanocomposite membranes using the vacuum infiltration technique. Figure 7 demonstrates the nanoporous membrane formation. Transmission electron microscopy and scanning electron microscopy images of the nanocomposite membranes were analyzed. The graphene oxide formed uniformly dispersed layered arrangements in the polymer matrix. Figure 8 displays the pore structure, size distribution, and morphology according to the transmission electron microscopy. Increasing nanofiller contents enhanced the graphene dispersion in the matrix. Moreover, the pore distribution and pore sizes were enhanced with the nanofiller loading. The grafting of polymer membrane with phosphotungstic acid formed homogeneous dispersion of nanofiller and polymer chain alignment. Hence, considerable research attempts have been observed regarding the polysulfone/graphene nanocomposite membranes for gas

separation. However, more research efforts must be performed on modified polysulfone matrix-based nanocomposite membranes that could enhance the selectivity and permeation through the membranes.

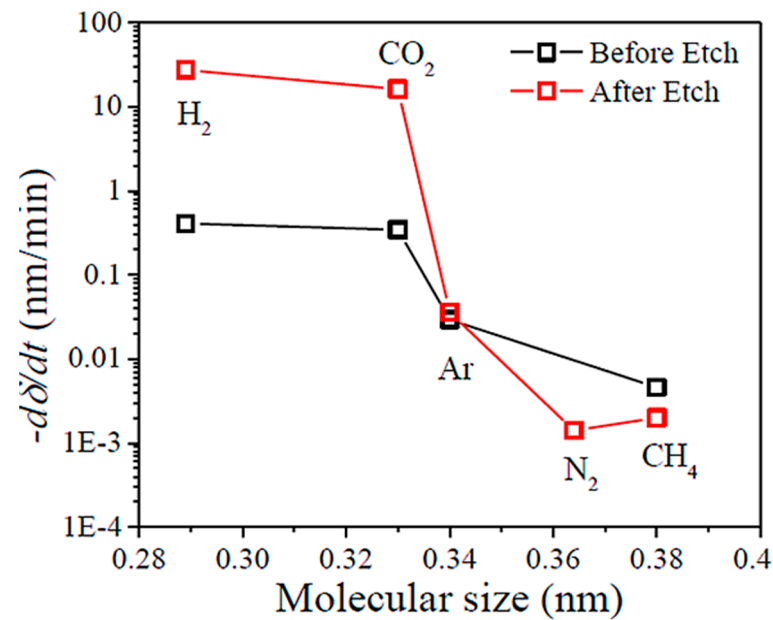


**Figure 5.** Comparing leak rates between pristine and porous graphene membranes [94]. Reproduced with permission from Nature.

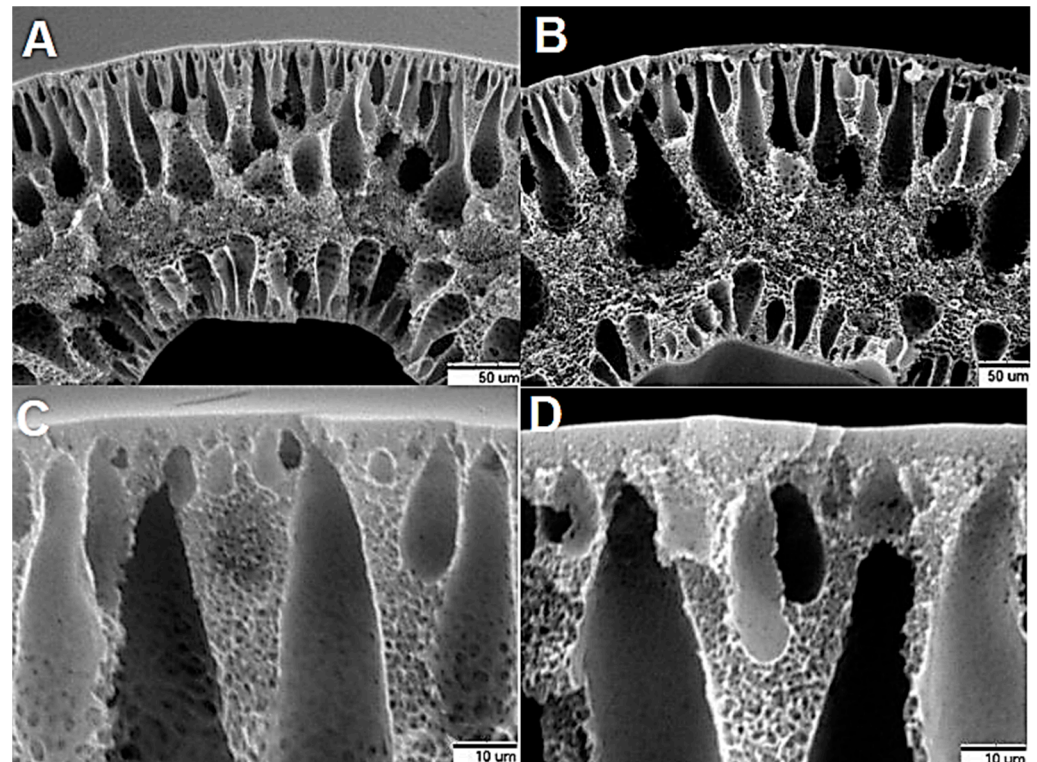


**Figure 6.** Scanning electron microscopy cross section images of (A) pristine polysulfone; (B) polysulfone/graphene oxide mixed matrix membrane (magnification  $\times 1.5k$ ); (C) pristine polysulfone; and (D) polysulfone/graphene oxide mixed matrix membrane (magnification  $\times 10k$ ) [105]. Reproduced with permission from Creative Commons Attribution 3.0 license.



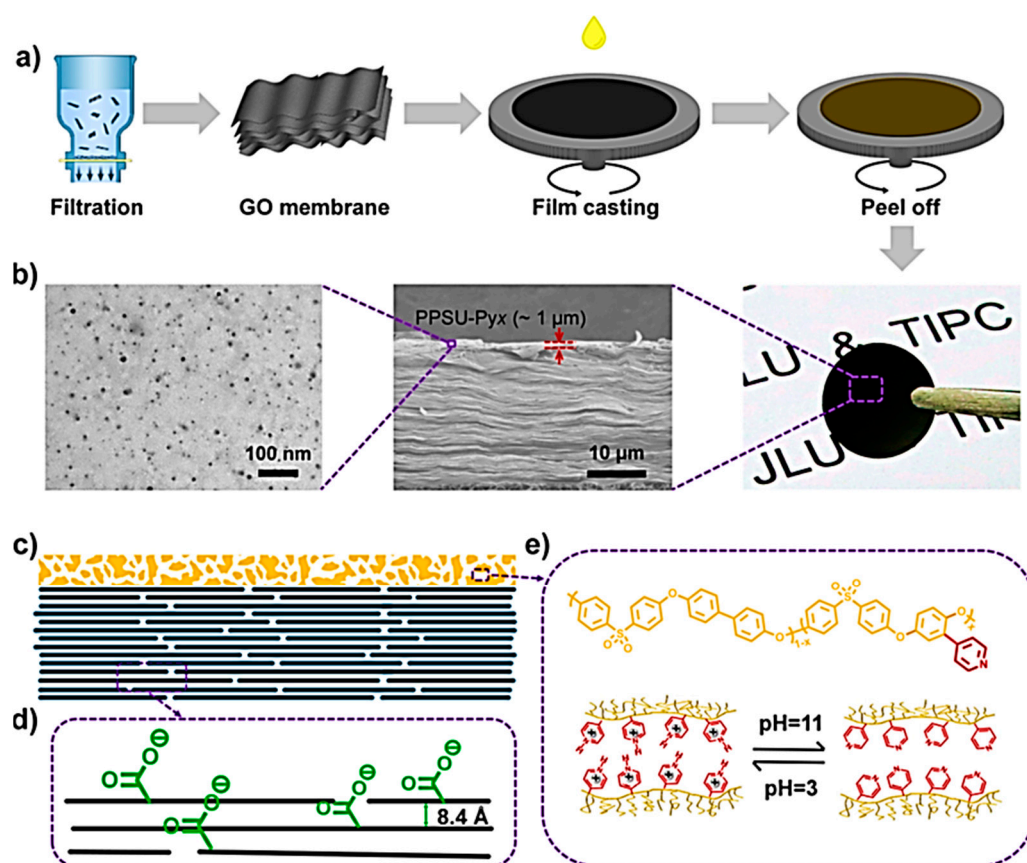


**Figure 7.** Schematic of heterogeneous membrane with asymmetric structure (a) fabrication process of membrane: copolymer spin-coated on GO nanosheets prepared by vacuum filtration; (b) transmission electron microscopy image of PPSU-Pyx that was marked with phosphotungstic acid (PTA); middle image is scanning electron microscopy observation of cross section of heterogeneous membrane; on right is photo of heterogeneous GO/PPSU-Pyx membrane; (c) schematic of heterogeneous structure with 3D pores (self-assembly into interconnected pores by ionomers) and 2D pores (self-assembly into nanosheets by GO); (d) illustration of GO nanosheets with spacing of ca. 0.84 nm; and (e) chemical structure of PPSU-Pyx (upper) and configuration change of polymer in response to pH (lower) [108]. PPSU-Pyx = polyphenylsulfone-pyridine; GO/PPSU-Pyx = graphene oxide/polyphenylsulfone-pyridine; GO = graphene oxide. Reproduced with permission from ACS.

Poly(dimethyl siloxane) has been applied as matrix materials for gas separation membranes [109–111]. The separation efficiency of these membranes was investigated for CO<sub>2</sub> and other gases. However, the ultrathin poly(dimethyl siloxane)-based membranes have the challenges of low gas permeance and weak interfacial properties [112]. Therefore, nanofillers have been incorporated in the poly(dimethyl siloxane) membranes to attain the desired gas separation properties. Berean et al. [113] prepared the poly(dimethyl siloxane)/graphene nanocomposites via solution route in p-xylene solvent. Graphene nanosheets were obtained through chemical vapor deposition. Ultrasonication was performed for better graphene dispersion and developing  $\pi$ - $\pi$  interactions between the matrix-nanofiller. Figure 9 shows a schematic of diffusion paths through the poly(dimethyl siloxane) and poly(dimethyl siloxane)/graphene nanocomposites, including graphene nanofiller in the matrix which led to interfacial voids and long diffusion paths formation for gaseous species. High passive surface and bulk diffusion of gas molecules through the neat poly(dimethyl siloxane) membrane were observed. On the other hand, the poly(dimethyl siloxane)/graphene nanocomposites have selective passive surface and bulk diffusion of gases due to dispersed graphene nanosheets. The 0.2 wt.% graphene loading revealed high gas permeation of up to 60% for N<sub>2</sub>, CO<sub>2</sub>, Ar, and CH<sub>4</sub>, relative to neat poly(dimethyl



siloxane) membrane. At this nanofiller content, better graphene dispersion and diffusion path formation were suggested. Moreover, the  $\text{CO}_2/\text{CH}_4$  selectivity of the nanocomposite membrane was found to be higher (4.2), compared with the neat polymeric membrane (3.6).

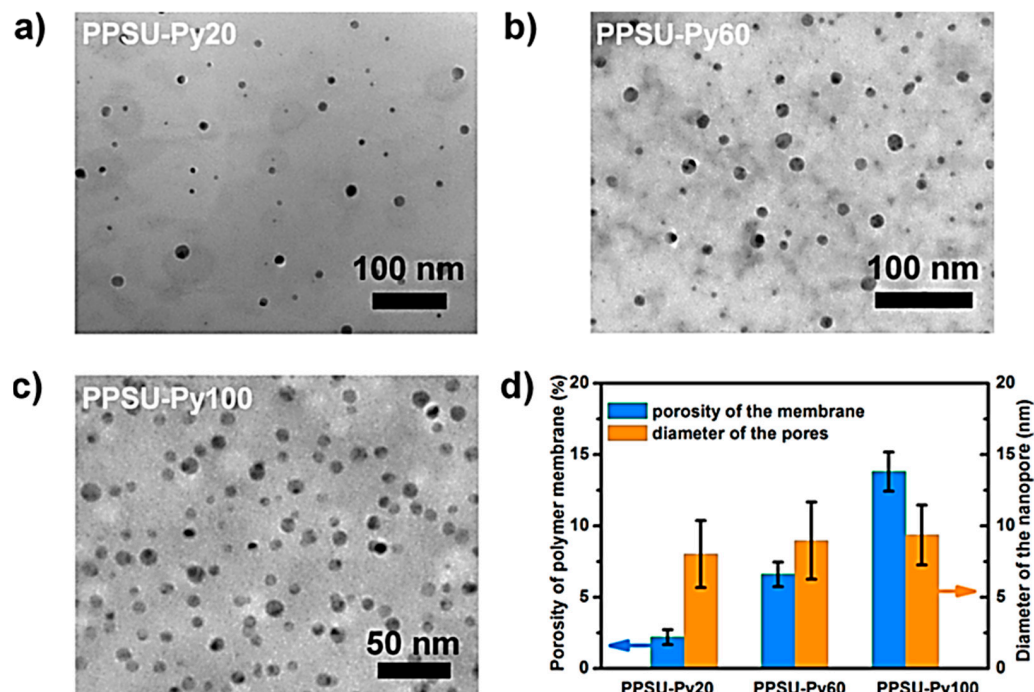


**Figure 8.** Pore structure and size distribution with different pyridine moiety proportions in PPSU-Pyx. (a–c) Transmission electron microscopy images of PPSU-Pyx. Dark areas refer to pores and white areas represent hydrophobic backbone along the copolymer chain. The polymer is marked with PTA, which reacted with pyridine moiety. (d) Porosity and diameter of copolymer membrane with different pyridine moiety proportions, indicating improved porosity while pore size stays almost the same [108]. PTA = phosphotungstic acid; PPSU-Pyx = polyphenylsulfone-pyridine; GO = graphene oxide. Reproduced with permission from ACS.

Koolivand et al. [114] designed the poly(dimethyl siloxane) and graphene oxide-based nanocomposite membranes. For this purpose, graphene oxide was prepared using Hummer's method [115]. Solution and ultrasonication methods were used for the fabrication of membranes in tetrahydrofuran solvent. Scanning electron microscopy and spectroscopic analysis have been used to study the interfacial interactions between the polymers and nanofillers. The poly(dimethyl siloxane)/graphene oxide nanocomposite membranes were investigated for the  $\text{CO}_2/\text{CH}_4$  separation and  $\text{CO}_2$  permeability. Including 5 wt.% graphene oxide contents resulted in high  $\text{CO}_2/\text{CH}_4$  selectivity at 112% and  $\text{CO}_2$  permeability at 29%. Ha et al. [116] also prepared the poly(dimethyl siloxane)/graphene oxide nanocomposite membrane using solution casting method in tetrahydrofuran solvent. Adding 8 wt.% graphene oxide reduced the permeability of  $\text{H}_2$ ,  $\text{O}_2$ ,  $\text{N}_2$ ,  $\text{CH}_4$  and  $\text{CO}_2$  gases by 99.9%. It was observed that the gas transportation and permeation properties were due to nanofiller dispersion in the matrix. Compared with the neat poly(dimethyl siloxane) membrane, the selectivity of gases ( $\text{CO}_2/\text{O}_2$ ,  $\text{CO}_2/\text{N}_2$ , and  $\text{CO}_2/\text{CH}_4$ ) was enhanced with the graphene oxide loadings and dispersion (Figure 10). Selectivity also depends upon the difference in kinetic diameters of  $\text{CO}_2/\text{O}_2$ ,  $\text{CO}_2/\text{N}_2$ , and  $\text{CO}_2/\text{CH}_4$  (0.16, 0.34, and 0.50 Å, respectively). Additionally, the successful research attempts, new poly(dimethyl siloxane)/graphene and poly(dimethyl siloxane)/graphene oxide nanocomposite membranes, need to be developed and studied. The morphological and interfacial properties of these membranes also need to be investigated for gas diffusion and separation mechanisms.

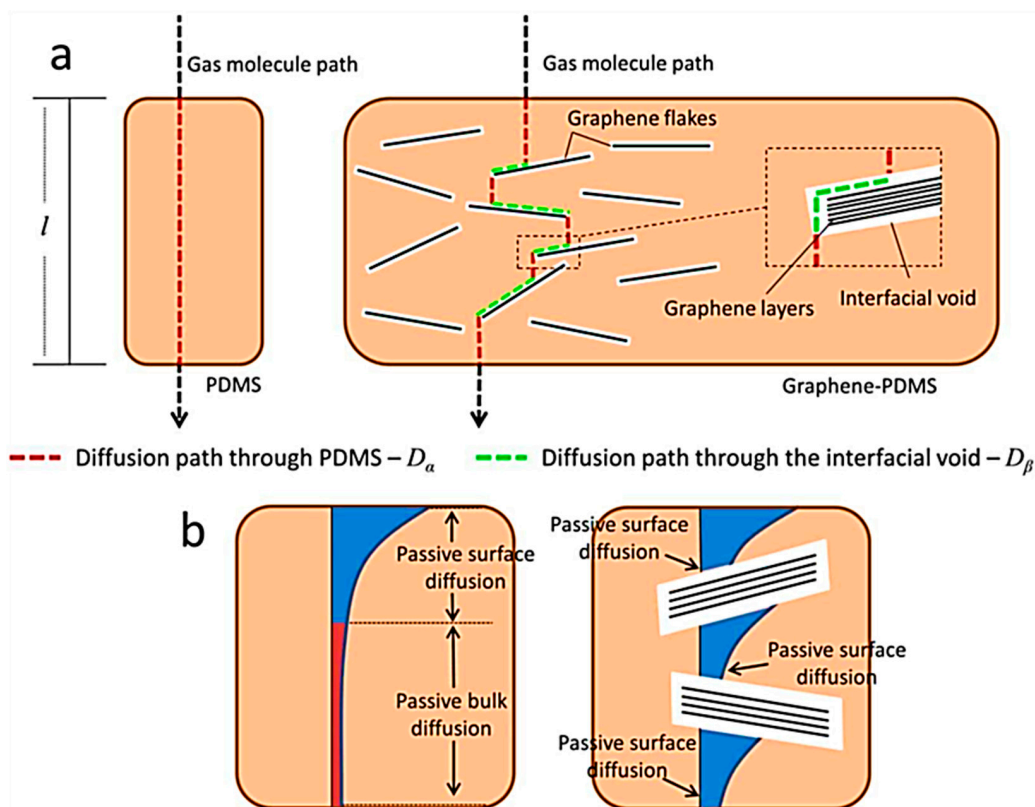


**Figure 9.** (a) Schematic of diffusion paths for PDMS and PDMS/graphene nanocomposites. The total path length for pristine PDMS membrane is  $l$ . In PDMS/graphene nanocomposite membrane, the diffusion path ( $D_\alpha$ ) is shown in red and the diffusion path through interfacial void ( $D_\beta$ ) is shown in green; (b) a schematic depicting the difference between passive surface and bulk diffusion of gas molecules in pristine PDMS and PDMS/graphene nanocomposite membranes [113]. PDMS = poly(dimethyl siloxane). Reproduced with permission from ACS.

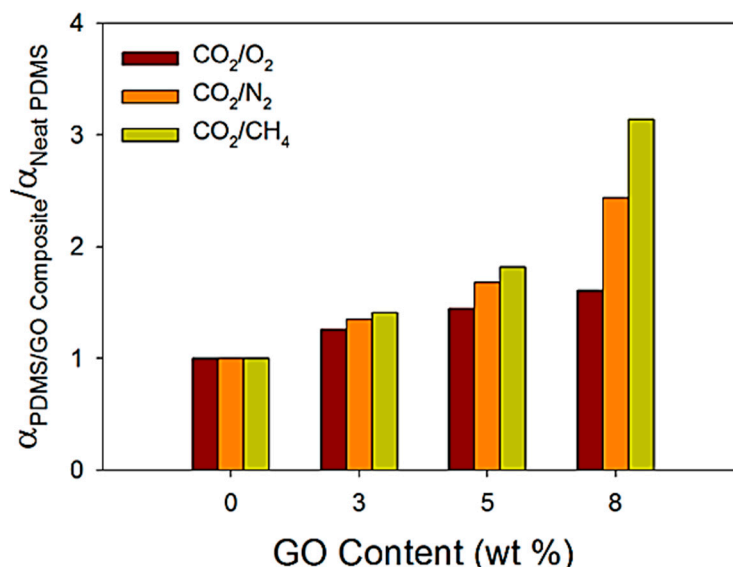


**Figure 10.** Relative ideal selectivity of CO<sub>2</sub> for poly(dimethyl siloxane)/graphene oxide nanocomposite [116]. Reproduced with permission from Elsevier.

Poly(methyl methacrylate) has been used as a matrix for gas separation membranes [117–119]. Baldanza et al. [120] fabricated the poly(methyl methacrylate)/

graphene nanocomposite membranes using wet deposition method. This technique involves the ‘lift-off/float-on’ process for developing membranes [121]. Single-layer graphene was grown using the chemical vapor deposition technique. Figure 11 shows the permeability coefficients measured for the pristine poly(methyl methacrylate) and poly(methyl methacrylate)/graphene nanocomposite membranes using pure and humidified CO<sub>2</sub> and O<sub>2</sub> (at different R.H. levels) (Table 2). It has been observed that including graphene nanofiller decreased the permeability coefficient of CO<sub>2</sub> and O<sub>2</sub> to  $1.30 \times 10^{-17}$  and  $0.21 \times 10^{-17}$  mol·m·m<sup>-2</sup>·Pa<sup>-1</sup>·s<sup>-1</sup>, respectively, compared with the neat polymeric membrane. Decreasing gas permeability was attributed to the formation of diffusion paths, due to graphene nanofiller dispersion in the matrix. The permeability coefficients of the gases were found comparable to the reported commercial poly(methyl methacrylate) membranes [122]. Few studies have been reported so far on poly(methyl methacrylate)/graphene nanocomposite-based gas separation membranes. Here, more focused research efforts are required in this field.

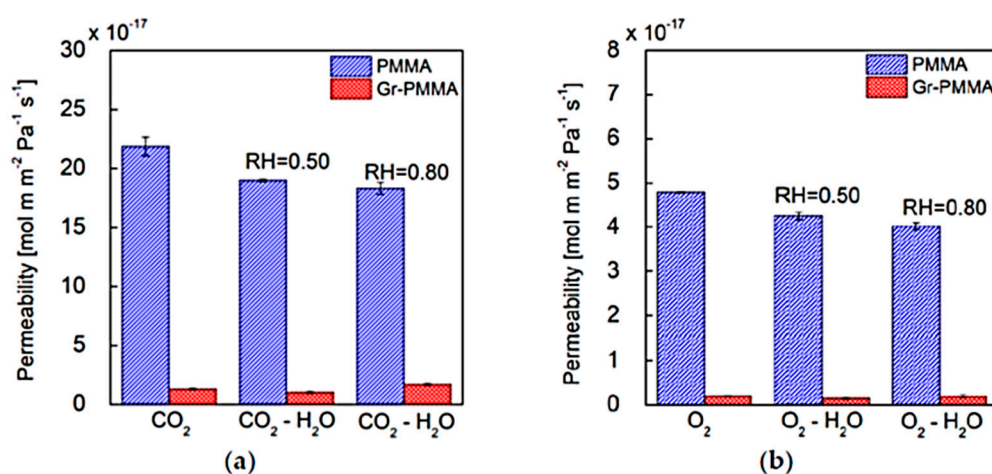


**Figure 11.** Gas permeability coefficients at 25 °C through poly(methyl methacrylate) (PMMA) (blue bars) and Gr-PMMA (poly(methyl methacrylate)/graphene nanocomposite) (red bars) for (a) CO<sub>2</sub> and humidified CO<sub>2</sub> and for (b) O<sub>2</sub> and humidified O<sub>2</sub> [120]. Reproduced with permission from MDPI.

**Table 2.** Permeability coefficients of CO<sub>2</sub> or O<sub>2</sub> through the nanocomposite at different R.H. levels [120]. PMMA = poly(methyl methacrylate); Gr-PMMA = poly(methyl methacrylate)/graphene nanocomposite). Reproduced with permission from MDPI.

| Nanolaminate/Permeating Gas | P [mol·m·m <sup>-2</sup> ·Pa <sup>-1</sup> ·s <sup>-1</sup> ] | P [Barrer]                         |
|-----------------------------|---|------------------------------------|
| PMMA/CO <sub>2</sub>        | $21.9 (\pm 0.8) \times 10^{-17}$                              | $6.5 (\pm 0.2) \times 10^{-1}$     |
| Gr-PMMA/CO <sub>2</sub>     | $1.30 (\pm 0.1) \times 10^{-17}$                              | $0.39 (\pm 0.03) \times 10^{-1}$   |
| PMMA/O <sub>2</sub>         | $4.79 (\pm 0.01) \times 10^{-17}$                             | $1.434 (\pm 0.003) \times 10^{-1}$ |
| Gr-PMMA/O <sub>2</sub>      | $0.21 (\pm 0.01) \times 10^{-17}$                             | $0.063 (\pm 0.003) \times 10^{-1}$ |

Polyimide-based nanocomposite membranes have been developed for gas separation [123–125]. Melicchio et al. [126] prepared the polyimide/graphene oxide nanocomposite membrane using a knife casting technique. The commercial polyimide Matrimid<sup>®</sup> 5218 was used as a matrix along with dimethylformamide solvent. Figure 12 shows the dispersion of graphene oxide nanoflakes in the polyimide chains. The graphene oxide nanoflakes were dispersed in a particular arrangement in the matrix that enhanced the polymer chain rigidity. Moreover, the nanofiller dispersion affected the membrane permeability properties. Figure 13 presents the gas permeability apparatus used in this study. Variable pressure of up to 70 bar was applied. The apparatus consists of a permeation cell, a high-pressure side, and a low-pressure side. Including 0.57 vol.% graphene oxide led to H<sub>2</sub> and CO<sub>2</sub> permeability of 28 and 8 Barrer, respectively. Moreover, the ideal selectivity (3.5) was observed for H<sub>2</sub>/CO<sub>2</sub>.

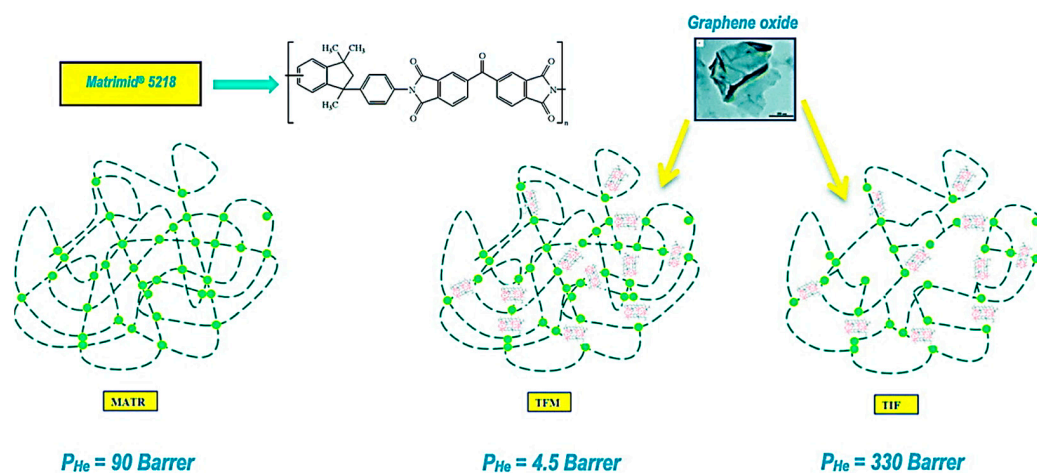


**Figure 12.** Possible configurations of graphene oxide nanofiller in polyimide membrane [126]. MATR = Matrimid<sup>®</sup> 5218; TFM = thin film membrane; TIF = thick isotropic film. Reproduced with permission from Elsevier.

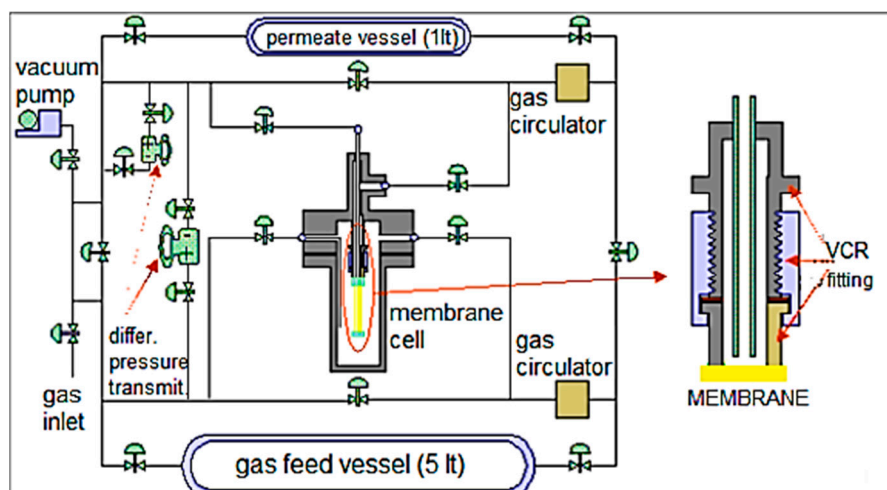


**Figure 13.** Gas permeability apparatus (operated from high vacuum up to 70 bar pressure conditions) [126]. Reproduced with permission from Elsevier.

The poly(1-trimethylsilyl-1-propyne) matrix was also used for the membrane formation [127–129]. Olivieri et al. [130] fabricated the poly(1-trimethylsilyl-1-propyne) and graphene oxide-based gas permeation membranes using chloroform solvent. Including 1 wt.% graphene led to better nanofiller dispersion and diffusion coefficient of 25% for CO<sub>2</sub>, 14% for N<sub>2</sub>, and 9% for CH<sub>4</sub>. Alberto et al. [131] also fabricated the poly(1-trimethylsilyl-1-propyne)/graphene nanocomposite membranes. The 0.05 wt.% loading revealed CO<sub>2</sub> permeability of  $3.5 \times 10^3$  Barrer. The permeability was 39% reduced compared with the neat polymeric membrane. However, few systems have been reported on the poly(1-trimethylsilyl-1-propyne)/graphene oxide membranes. Poly(2,6-dimethyl-1,4-phenylene oxide) has also been used as a matrix for these membranes [132–134]. Rea and co-workers [135] designed the poly(2,6-dimethyl-1,4-phenylene oxide)/graphene membrane with 0.3–15 wt.% nanofiller contents. Figure 14 presents the permeability values with increasing graphene loading, at 35 and 65 °C. Increasing nanofiller loading level reduced the gas permeability. A decrease in permeability was observed due to nanofiller dispersion and development of a polymer-nanofiller interphase. Graphene nanoparticles formed diffusion pathways for the controlled permeation of gas molecules.



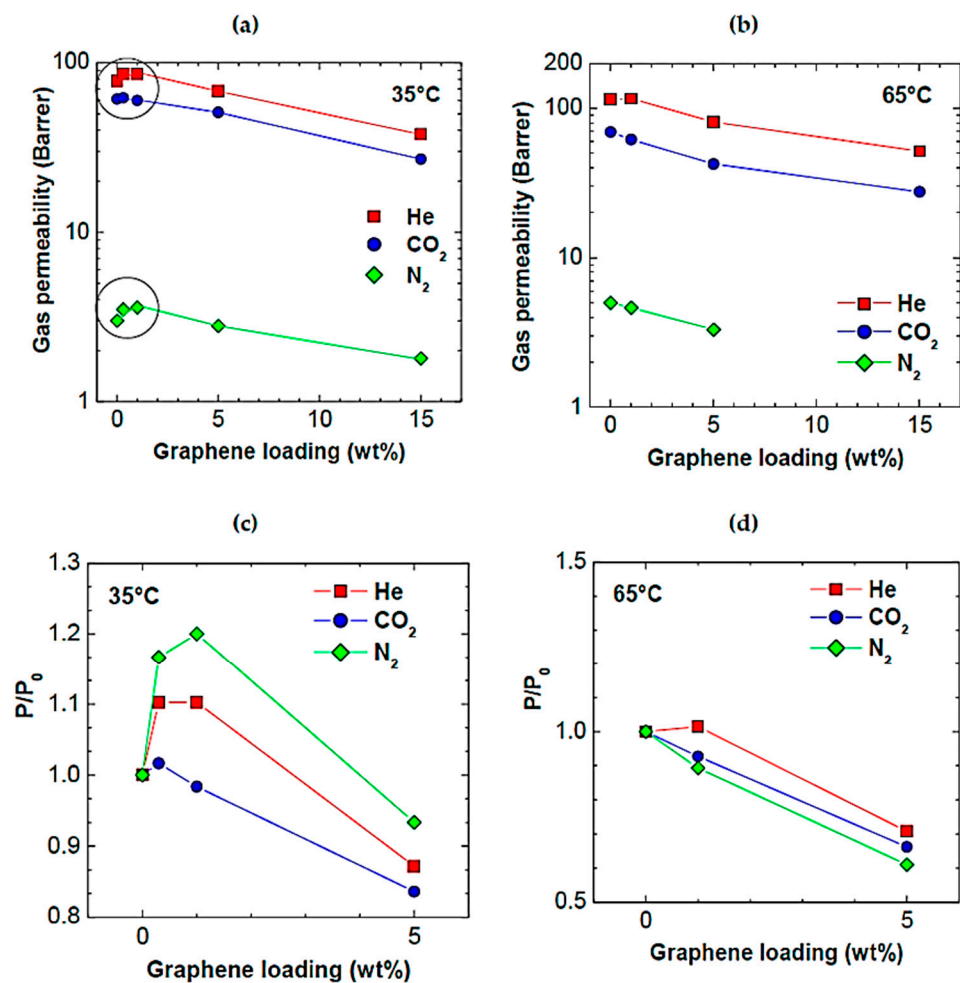


**Figure 14.** Gas permeability before (a) 35 °C; (b) 65 °C; and after graphene addition (c) 35 °C; (d) 65 °C, as a function of graphene loading in poly(1-trimethylsilyl-1-propyne) matrix [135]. Reproduced with permission from MDPI.

Numerous polymer/graphene and polymer/graphene oxide nanocomposite membranes have been designed for gas separation (Table 3) [136]. Graphene and graphene oxide nanofillers have been reinforced in polymeric matrices such as polysulfone, polyphenylsulfonopyridine, poly(dimethyl siloxane), poly(methyl methacrylate), polyimide, poly(1-trimethylsilyl-1-propyne), poly(2,6-dimethyl-1,4-phenylene oxide), cellulose, etc., for developing nanocomposite membranes. Among facile techniques for membrane fabrication, solution casting, ultrasonication, wet deposition, phase inversion, dry-wet phase inversion, vacuum infiltration, and knife casting approaches have been successfully used. The resulting membranes have high porosity, selectivity, permeability, and other superior properties. Moreover, these membranes revealed fine interfacial interactions, matrix-nanofiller interlinking, microstructure, nanofiller dispersion, hydrophobicity, water absorption, wettability, contact angle, response to pH, chemicals, moisture, flexibility, and mechanical properties. Dispersion and alignment of graphene or graphene oxide nanoparticles in membranes enhanced the selective permeation of gas molecules. The polymer/graphene nanocomposite membrane designs need to be further improved for separating complex gas mixtures.



**Table 3.** Specifications of polymer/graphene nanocomposite membranes for gas separation.

| Polymer                          | Nanofiller                 | Fabrication Route  | Physicochemical Properties   | Membrane Properties  | Ref.  |
|----------------------------------|----------------------------|--|--|--|-------|
| Polymer                          | Graphene or graphene oxide | Solution casting   | Ion-molecule interaction; 1.8–20 nm thickness  | H <sub>2</sub> /N <sub>2</sub> selectivity 900; H <sub>2</sub> /CO <sub>2</sub> selectivity 3400; pore size ~0.34 nm   | [96]  |
| Polysulfone                      | Graphene oxide             | Dry-wet phase inversion techniques; dimethyl acetamide solvent; hollow fiber mixed matrix membrane | Graphene oxide own $\pi$ - $\pi$ stacking form interaction with CO <sub>2</sub> gas and polar gas molecules; multi-layered porous structure with large macro-voids   | 0.25 wt.% nanofiller; CO <sub>2</sub> /CH <sub>4</sub> separation 25; CO <sub>2</sub> permeance 86.80 GPU  | [105] |
| Polysulfone                      | Graphene                   | Phase inversion; hollow fiber mixed matrix membrane  | Nanosize synthesized graphene; interfacial interaction between graphene and polymer matrix   | CO <sub>2</sub> /N <sub>2</sub> selectivity 158%; CO <sub>2</sub> /CH <sub>4</sub> selectivity 74%   | [106] |
| Polysulfone                      | Graphene oxide             | Solution route; N-Methyl-2-pyrrolidone solvent   | Physical interaction between oxygenated functional groups of graphene oxide and polymer; interactions between functional groups of nanocomposites and gas molecules  | CO <sub>2</sub> /CH <sub>4</sub> selectivity ~45   | [107] |
| Polyphenylsulfone-pyridine       | Graphene oxide             | Vacuum infiltration technique  | Wettability and surface charge response to pH; acidic pH = 3 form hydrophilic state contact angle 63.3°; alkaline pH = 11 form hydrophobic state contact angle 106.5°; charge-density-tunable nanoporous; power of $\approx 0.76 \text{ W m}^{-2}$ | Dispersion; morphology   | [108] |
| Poly(dimethyl siloxane)          | Graphene                   | Solution casting; p-xylene solvent   | $\pi$ - $\pi$ interactions in matrix-nanofiller  | 0.2 wt.% nanofiller; N <sub>2</sub> , CO <sub>2</sub> , Ar, and CH <sub>4</sub> permeation 60%; CO <sub>2</sub> /CH <sub>4</sub> selectivity 4.2   | [113] |
| Poly(dimethyl siloxane)          | Graphene oxide             | Solution/ultrasonication methods; tetrahydrofuran solvent  | Interfacial interactions between functional groups of graphene oxide and polymer; density 1.09–1.12; thickness 1.9–2.8 nm  | 5 wt.% nanofiller; CO <sub>2</sub> /CH <sub>4</sub> selectivity 112%; CO <sub>2</sub> permeability 29%   | [114] |
| Poly(dimethyl siloxane)          | Graphene oxide             | Solution casting   | Matrix-nanofiller interactions; interaction between graphene oxide and polymer   | 8 wt.% nanofiller; H <sub>2</sub> , O <sub>2</sub> , N <sub>2</sub> , CH <sub>4</sub> and CO <sub>2</sub> permeability 99.9%   | [116] |
| Poly(methyl methacrylate)        | Graphene                   | Wet deposition method  | Water adsorption; membrane wrinkles; degree of dispersion/orientation of the graphene nanosheet; structure organization of polymeric chains at the interface with graphene nanosheet   | CO <sub>2</sub> permeability coefficient $1.30 \times 10^{-17} \text{ mol}\cdot\text{m}\cdot\text{m}^{-2}\cdot\text{Pa}^{-1}\cdot\text{s}^{-1}$ ; O <sub>2</sub> permeability coefficient $0.21 \times 10^{-17} \text{ mol}\cdot\text{m}\cdot\text{m}^{-2}\cdot\text{Pa}^{-1}\cdot\text{s}^{-1}$ | [120] |
| Polyimide                        | Graphene oxide             | Knife casting technique  | Graphene oxide nanoflake anchoring; polymer-graphene interphasedensity; water and testing gas sorption   | 0.57 vol.% nanofiller; H <sub>2</sub> permeability 28 Barrer; CO <sub>2</sub> permeability 8 Barrer; H <sub>2</sub> /CO <sub>2</sub> selectivity 3.5   | [126] |
| Poly(1-trimethylsilyl-1-propyne) | Graphene oxide             | Solution casting; chloroform solvent   | Anchoring of graphene oxide nanosheets lowers membrane flexibility; less free volume; covalent cross-linking of polymer  | 1 wt.% graphene; diffusion coefficient of CO <sub>2</sub> (25%); N <sub>2</sub> (14); CH <sub>4</sub> (9%)   | [130] |
| Poly(1-trimethylsilyl-1-propyne) | Graphene                   | Solution route   | Interaction between filler and polymer matrix; 0.93–1.36 MPa; 38–44 MPa  | 0.05 wt.% nanofiller; CO <sub>2</sub> permeability $3.5 \times 10^3$ Barrer  | [131] |

Table 3. Cont.

| Polymer                                | Nanofiller     | Fabrication Route | Physicochemical Properties   | Membrane Properties  | Ref.  |
|--|----------------|-------------------|--|--|-------|
| Poly(2,6-dimethyl-1,4-phenylene oxide) | Graphene       | Solution route    | Void formation at interface; glassy polymer filled with graphene; graphene inclusion for physical constraint to relaxation of polymer chains | 0.3–15 wt.% nanofiller reduced permeability  | [135] |
| Cellulose                              | Graphene oxide | Solution route    | Graphene oxide exfoliation in polymer; physical interactions; tensile strength and Young's modulus increase by 2 and 57 times, respectively  | 3.66 vol.% nanofiller; oxygen permeability coefficient $1.4 \times 10^{-17} \text{ cm}^3 \text{ cm} \cdot \text{cm}^{-2} \text{ s}^{-1} \text{ Pa}^{-1}$ | [137] |

### 5. Polymer/Graphene Nanofibers in Membrane Technology

The polymer nanofibers have been used for developing nanofibrous membranes [138]. In this context, thermoplastic polymers including polyamide, polystyrene, polyacrylonitrile, polyester, and various copolymers have been used [139]. Pristine polymer nanofibers have light weight, mechanical stability, thermal stability, chemical constancy, and environmental stability properties [140]. Due to superior physical characteristics, polymer nanofibers have been applied in membranes, coatings/films, packages, textiles, and biomedical devices [141]. Nanofillers have been reinforced to form the nanocomposite nanofibers having enhanced physical properties such as mechanical, thermal, chemical, and environmental stability [142]. An important application of polymer nanocomposite nanofibers has been observed for developing membranes [143]. In this way, graphene reinforced polymer nanocomposite nanofibers with superior mechanical and physical properties have been fabricated [144,145].

The polymer/graphene nanocomposite nanofibers have been fabricated using numerous efficient techniques such as electrospinning [146], wet spinning [147], melt spinning [148], etc. Spinning techniques have been effectively applied to attain uniform graphene nanoparticle dispersion in nanofibers. For graphene-based nanocomposite nanofibers, electrospinning has been found as a widely used and effective method [149]. Choice of manufacturing technique, type of polymer, graphene derivative, solvent, concentration, flow rate, applied field and other process parameters, and physicochemical properties affect the morphology, diameter, and applications of the nanofibers. It is important to analyze the effect of manufacturing techniques on nanofiber properties. Consequently, the graphene-based nanofiber properties including flexibility, tensile strength, modulus, thermal properties, hydrophobicity, chemical features, and other physical properties have been investigated [150]. The applications of polymer/graphene nanocomposite nanofibers have been observed in defense textiles, tissue engineering, sensors/actuators, etc. [151].

The polymer/graphene nanofibrous membranes having enhanced electrical conductivity, mechanical strength, heat stability, permeation, selectivity, and antimicrobial properties have been fabricated [152]. Nevertheless, polymer/graphene nanofibrous membranes have been less explored for the gas separation application, as compared to other technical applications [153]. Ren et al. [137] prepared the cellulose/graphene oxide nanocomposite nanofibers having ultra-low gas permeability properties. According to morphology analysis, nanofiller nanoparticles were uniformly dispersed and oriented in the nanofiber matrix. Consequently, the 3.66 vol.% graphene oxide contents reduced the oxygen permeability coefficient of the cellulose nanofibers ( $5.5 \times 10^{-13} \text{ cm}^3 \text{ cm} \cdot \text{cm}^{-2} \text{ s}^{-1} \text{ Pa}^{-1}$ ) to  $1.4 \times 10^{-17} \text{ cm}^3 \text{ cm} \cdot \text{cm}^{-2} \text{ s}^{-1} \text{ Pa}^{-1}$  in the nanocomposite nanofibers. Developing polymer/graphene nanofibers enhanced the surface area and interactions with gas molecules for separation. Moreover, Young's modulus of the cellulose/graphene oxide nanocomposite nanofibers was 57% higher than the neat cellulose nanofibers. Accordingly, high-performance polymer/graphene nanofibrous membranes were used for gas permeability applications.

Since the 20th century, the production of nanofiber-based membranes has been focused [154]. Progress in the 21st century (since the 2000s) has made fiber processes more commercially viable. Recent progress must focus on improving the current manufacturing technologies to produce nanofibers with high product consistency and process speed. Consequently, a large number of contract manufacturers can trade successfully. For efficient trading and commercial viability of nanofibers for technical applications, fibers having a fine diameter must be produced and be employed in industries.

Consequently, the polymer/graphene nanofibers have a homogeneous surface, large surface area-to-volume ratio, optimum porosity, flexibility, toughness, and mechanical strength for membrane application. Depending upon the polymer type and nanofiller used, physical and chemical properties of nanofibrous membranes can be varied.

## 6. Advantages/Shortcomings of Graphene Nanocomposites in Membrane Technology

Table 4 shows a comparative performance of graphene, graphene oxide, carbon nanotube, and inorganic nanofillers in polymeric gas separation membranes. Two-dimensional graphene-based materials revealed significance in the formation of new nanocomposite membranes for gas separation. The planar structure has been found suitable for the fabrication of thin selective layers at low nanofiller loadings. Increasing nanofiller loading enhanced the CO<sub>2</sub> permeability. The CO<sub>2</sub> selectivity properties also increased with the nanofiller contents. Using graphene-based membranes revealed high stability and intrinsic capabilities for varying polymer chain packing and increased permeability. Surface modification of graphene and derivatives offered an efficient approach for improving matrix-nanofiller interactions and CO<sub>2</sub> philicity. However, challenges exist in up-scaling of ultra-thin defect free selective nanocomposites and achieving fine compatibility.

There are several advantages of using graphene nanofiller in polymer nanocomposite membranes, compared with other nanofillers [155]. Adding graphene could result in lightweight and high-strength nanocomposites. Compared with other nanocarbons, graphene has a unique atomically thin structure and larger lateral dimensions [156]. Pristine graphene has been used as a promising nanomaterial in liquid barrier applications. Aligned graphene nanosheets restrict the diffusion of very small liquid molecules through selective permeation. Graphene and its derivatives have fine capability for developing ion-selective membranes [157]. Graphene oxide nanosheets possess large interlayer distance and empty spaces in polymers, compared with carbon nanotube and other nanocarbon nanofillers. Molecular simulation studies have been reported on graphene-based permeation membranes [158].

**Table 4.** Gas separation performance of graphene, carbon nanotube, and inorganic nanofillers based membranes.

| Polymer                             | Nanofiller       | Loading (wt.%) | PCO <sub>2</sub> (Barrer) | $\alpha$ CO <sub>2</sub> /CH <sub>4</sub> | Refs. |
|-------------------------------------|------------------|----------------|---------------------------|---|-------|
| Polyether ether ketone (PEEK)       | Graphene         | 0–6            | 292.6–565.3               | 38.1–42.8                                 | [159] |
| Polyethylene glycol                 | Graphene oxide   | 0.5–3          | 254.2–299.6               | 48.2–59.3                                 | [160] |
| Polysulfone                         | Graphene oxide   | 0–0.25         | 65.2–74.5                 | 17.3–44.4                                 | [106] |
| Polyethylene glycol-polyether imide | Graphene oxide   | 0–10           | 81.9–146                  | 18.7–24.4                                 | [161] |
| Polyethylene glycol                 | Carbon nanotube  | 0–2            | 23.5–35                   | 18.7–22.7                                 | [162] |
| Polyether sulfone                   | Carbon nanotube  | 0–10           | 2.6–4.4                   | 11.5–22                                   | [163] |
| Polysulfone                         | Carbon nanotube  | 0–15           | 3.9–4.52                  | 16.1–22.9                                 | [164] |
| Polyether sulfone                   | TiO <sub>2</sub> | 0–10           | 2–2.9                     | 14–15                                     | [165] |
| Polysulfone                         | Magnesium oxide  | 0–10           | 7.7–9.4                   | 25.4–27.7                                 | [166] |
| Polyimide                           | SiO <sub>2</sub> | 0–0.92         | 9.9–21.3                  | 33.2–36.6                                 | [167] |

Using polymeric membranes with nanofillers such as carbon nanotube, metal oxides, and other inorganic nanoparticles possess the disadvantages of high toxicity, high cost, and processability [168–170]. On the other hand, graphene nanocomposites have the advantages of better flexibility, structural stability, and environmental friendliness, and of not using toxic solvents. The polymer/graphene nanocomposites have fine nanofiller dispersion and alignment in matrices facilitating the gas molecules diffusion, selectivity, and barrier properties. Nevertheless, numerous disadvantages of graphene nanocomposites have been reported such as nanofiller aggregation and dispersion. Major limitations in the membrane separation processes were identified as fouling, shrinkage, and hydrophobicity [171]. Fouling is the phenomena of deposition of molecules inside the pores of membranes. This could decrease the durability, permeation, selectivity, and membrane life. Hydrophobicity of membranes has been found responsible for fouling. In general, polymeric membranes are hydrophobic due to a lack of a functional group in the backbone [172]. Graphene surface needs to be functionalized for better dispersion in polymers and to form compatible matrix-nanofiller interfaces. For this purpose, graphene oxide and modified graphene nanostructures have been designed to form functional membrane nanomaterials since few combinations of polymer/graphene membranes have been developed. Here, an exploration of structure-property relationships of polymer-graphene will be essential for future developments in this field [173].

## 7. Prospects and Summary

Several current challenges need to be overcome to attain progress in the field of polymer/graphene nanocomposite membranes. Few polymer/graphene designs have been developed for gas separation. In this context, numerous polymers still need to be explored for gas permeation membrane applications. New polymer/graphene design innovations could have remarkable morphology, mechanical/thermal stability, and superior gas separation performance. Moreover, better graphene dispersion is a challenging factor for developing high-performance polymer/graphene nanocomposite membranes. The graphene nanoparticle dispersion and matrix-nanofiller interactions could directly influence the pore size, shape, pore distribution, surface roughness, and membrane properties. In this context, using functional graphene could form advanced membrane systems with better nanoparticle dispersion and physical features.

The development of graphene oxide and other graphene derivative-based membranes could offer extremely high fluxes due to a thin nanostructure. In addition, graphene derivatives could result in high selectivity due to fine molecular sieving and narrow pore size distribution. Using modified graphene nanostructures could result in the optimum transportation of desired molecules through the membranes. Thus, graphene derivative membranes can be engineered using advanced ways to improve the membrane performance.

Graphene derivative-supported membranes can be fabricated using facile techniques through deposition of graphene derivative on support materials (porous polymers, porous ceramic, porous metal, etc.). Graphene-derived forms could offer enhanced gas separation performance and selectivity of the membrane support materials. Moreover, supported membranes have better porosity, thickness, wettability, and compatibility with the environment. Controlled thicknesses of nanocomposite-supported materials could promote gas transport and flux through the membranes. Consequently, self-standing ultrathin graphene derivative membranes can be developed having better separation performance, mechanical stability, and robustness.

Polymer nanocomposite graphene derivative membrane can be an emerging technology to attain higher permeability and higher selectivity than the pristine polymeric membranes. However, preparing mechanically stable ultrathin polymer/graphene-based nanocomposite membranes could be challenging.

Moreover, graphene-based membranes with interlayer spacing of  $< 1$  nm must be developed. This approach had enhanced the intercalation of gaseous molecules. This

method could enhance the specific gas separation performance of the graphene-based membranes.

Another challenge identified is large-scale processing of the polymer/graphene nanocomposite membranes for gas separation systems. In this context, a choice of suitable fabrication process and optimum processing conditions are important. Future efforts on developing polymer/graphene nanocomposite nanofibrous membranes are necessary for progress in the field of gas separation membranes. Advanced nanofibrous membranes could resolve the morphological, mechanical, barrier, selectivity, and permeability challenges regarding the polymer/graphene nanomaterials. Thus, advanced polymer/graphene designs, nanofiller dispersion, and fabrication techniques control the morphological, mechanical, durability, and gas transportation properties of the resulting membranes.

Henceforth, design and gas separation performance of the polymer/graphene nanocomposite membranes have been discussed in this state-of-the-art review. Graphene and modified graphene nanofillers have been reinforced in various polymeric matrices for developing nanocomposite membranes. Numerous research efforts have been observed regarding the design, structure, morphology, sturdiness, porosity, and gas separation efficiency of the polymer/graphene nanocomposite membranes. A choice of polymer, nanofiller modification, nanofiller dispersion, polymer-nanocarbon interactions, and fabrication strategies could be important to broaden the scope of these nanocomposite membranes and resolve the performance challenges.

**Author Contributions:** Conceptualization, A.K.; data curation, A.K.; writing of original draft preparation, A.K.; review and editing, A.K., I.A., T.Z., O.A. and M.H.E. All authors have read and agreed to the published version of the manuscript.

**Funding:** The authors extend their appreciation to the Deanship of Scientific Research at Imam Mohammad Ibn Saud Islamic University for funding this work through Research Group no. RG-21-09-49.

**Acknowledgments:** The authors acknowledge the support of the Deanship of Scientific Research at Imam Mohammad Ibn Saud Islamic University for supporting this work.

**Conflicts of Interest:** The authors declare no conflict of interest.

## References

1. Vroulias, D.; Staurianou, E.; Ioannides, T.; Deimede, V. Poly (ethylene oxide)-Based Copolymer-IL Composite Membranes for CO<sub>2</sub> Separation. *Membranes* **2022**, *13*, 26. [[CrossRef](#)]
2. Liu, Y.; Li, N.; Cui, X.; Yan, W.; Su, J.; Jin, L. A Review on the Morphology and Material Properties of the Gas Separation Membrane: Molecular Simulation. *Membranes* **2022**, *12*, 1274. [[CrossRef](#)]
3. Kausar, A.; Ahmad, I.; Maaza, M.; Eisa, M. State-of-the-Art of Polymer/Fullerene C60 Nanocomposite Membranes for Water Treatment: Conceptions, Structural Diversity and Topographies. *Membranes* **2023**, *13*, 27. [[CrossRef](#)]
4. Park, J.M.; Cao, Y.; Xia, L.-Q.; Sun, S.; Watanabe, K.; Taniguchi, T.; Jarillo-Herrero, P. Robust superconductivity in magic-angle multilayer graphene family. *Nat. Mater.* **2022**, *21*, 877–883. [[CrossRef](#)] [[PubMed](#)]
5. Yang, E.; Goh, K.; Chuah, C.Y.; Wang, R.; Bae, T.-H. Asymmetric mixed-matrix membranes incorporated with nitrogen-doped graphene nanosheets for highly selective gas separation. *J. Membr. Sci.* **2020**, *615*, 118293. [[CrossRef](#)]
6. Javed, R.M.N.; Al-Othman, A.; Tawalbeh, M.; Olabi, A.G. Recent developments in graphene and graphene oxide materials for polymer electrolyte membrane fuel cells applications. *Renew. Sustain. Energy Rev.* **2022**, *168*, 112836. [[CrossRef](#)]
7. Chumakova, N.A.; Kalai, T.; Rebrikova, A.T.; Sár, C.; Kokorin, A.I. Novel Orientation-Sensitive Spin Probes for Graphene Oxide Membranes Study. *Membranes* **2022**, *12*, 1241. [[CrossRef](#)] [[PubMed](#)]
8. Liu, Q.; Yang, Z.; Liu, G.; Sun, L.; Xu, R.; Zhong, J. Functionalized GO Membranes for Efficient Separation of Acid Gases from Natural Gas: A Computational Mechanistic Understanding. *Membranes* **2022**, *12*, 1155. [[CrossRef](#)]
9. Favre, E. Membrane Separation Processes and Post-Combustion Carbon Capture: State of the Art and Prospects. *Membranes* **2022**, *12*, 884. [[CrossRef](#)]
10. Lee, J.; Park, C.-Y.; Kong, C.-I.; Lee, J.-H.; Moon, S.-Y. Ultrathin Water-Cast Polymer Membranes for Hydrogen Purification. *ACS Appl. Mater. Interfaces* **2022**, *14*, 7292–7300. [[CrossRef](#)] [[PubMed](#)]
11. Pal, N.; Saini, N.; Agarwal, M.; Awasthi, K. Experimental investigation of natural polysaccharide-based mixed matrix membrane modified with graphene oxide and Pd-nanoparticles for enhanced gas separation performance. *Int. J. Hydrogen Energy* **2022**, *47*, 41820–41832. [[CrossRef](#)]



12. Mohsenpour, S.; Leaper, S.; Shokri, J.; Alberto, M.; Gorgojo, P. Effect of graphene oxide in the formation of polymeric asymmetric membranes via phase inversion. *J. Membr. Sci.* **2022**, *641*, 119924. [[CrossRef](#)]
13. He, X.; Ou, D.; Wu, S.; Luo, Y.; Ma, Y.; Sun, J. A mini review on factors affecting network in thermally enhanced polymer composites: Filler content, shape, size, and tailoring methods. *Adv. Compos. Hybrid Mater.* **2022**, *5*, 21–38. [[CrossRef](#)]
14. Fatemi, S.M.; Fatemi, S.J.; Abbasi, Z. Gas separation using graphene nanosheet: Insights from theory and simulation. *J. Mol. Model.* **2020**, *26*, 322. [[CrossRef](#)]
15. Liu, M.; Cen, R.; Zhao, J.; Yu, Z.-C.; Chen, L.-X.; Li, Q.; Tao, Z.; Xiao, X. Selective gradient separation of aminophenol isomers by cucurbit [6] uril. *Sep. Purif. Technol.* **2023**, *304*, 122342. [[CrossRef](#)]
16. Bahri, M.; Gebre, S.H.; Elaguech, M.A.; Dajan, F.T.; Sendeku, M.G.; Tlili, C.; Wang, D. Recent advances in chemical vapour deposition techniques for graphene-based nanoarchitectures: From synthesis to contemporary applications. *Coord. Chem. Rev.* **2023**, *475*, 214910. [[CrossRef](#)]
17. Raza, A.; Hassan, J.Z.; Mahmood, A.; Nabgan, W.; Ikram, M. Recent advances in membrane-enabled water desalination by 2D frameworks: Graphene and beyond. *Desalination* **2022**, *531*, 115684. [[CrossRef](#)]
18. Zhang, W.; Xu, H.; Xie, F.; Ma, X.; Niu, B.; Chen, M.; Zhang, H.; Zhang, Y.; Long, D. General synthesis of ultrafine metal oxide/reduced graphene oxide nanocomposites for ultrahigh-flux nanofiltration membrane. *Nat. Commun.* **2022**, *13*, 471. [[CrossRef](#)] [[PubMed](#)]
19. Lecaros, R.L.G.; Matira, A.R.; Tayo, L.L.; Hung, W.-S.; Hu, C.-C.; Tsai, H.-A.; Lee, K.-R.; Lai, J.-Y. Homostructured graphene oxide-graphene quantum dots nanocomposite-based membranes with tunable interlayer spacing for the purification of butanol. *Sep. Purif. Technol.* **2022**, *283*, 120166. [[CrossRef](#)]
20. Liu, Y.; Wang, X.; Gao, X.; Zheng, J.; Wang, J.; Volodin, A.; Xie, Y.F.; Huang, X.; Van der Bruggen, B.; Zhu, J. High-performance thin film nanocomposite membranes enabled by nanomaterials with different dimensions for nanofiltration. *J. Membr. Sci.* **2020**, *596*, 117717. [[CrossRef](#)]
21. Nidamanuri, N.; Li, Y.; Li, Q.; Dong, M. Graphene and graphene oxide-based membranes for gas separation. *Eng. Sci.* **2020**, *9*, 3–16. [[CrossRef](#)]
22. Rehman, F.; Memon, F.H.; Bhatti, Z.; Iqbal, M.; Soomro, F.; Ali, A.; Thebo, K.H. Graphene-based composite membranes for isotope separation: Challenges and opportunities. *Rev. Inorg. Chem.* **2022**, *42*, 327–336. [[CrossRef](#)]
23. Kononova, S.V.; Gubanov, G.N.; Korytkova, E.N.; Sapegin, D.A.; Setnickova, K.; Petrychkovych, R.; Uchytel, P. Polymer nanocomposite membranes. *Appl. Sci.* **2018**, *8*, 1181. [[CrossRef](#)]
24. Priya, A.; Gnanasekaran, L.; Kumar, P.S.; Jalil, A.; Hoang, T.K.; Rajendran, S.; Soto-Moscoso, M.; Balakrishnan, D. Recent trends and advancements in nanoporous membranes for water purification. *Chemosphere* **2022**, *303*, 135205. [[CrossRef](#)] [[PubMed](#)]
25. Ahmad, A.; Tariq, S.; Zaman, J.U.; Perales, A.I.M.; Mubashir, M.; Luque, R. Recent trends and challenges with the synthesis of membranes: Industrial opportunities towards environmental remediation. *Chemosphere* **2022**, *306*, 135634. [[CrossRef](#)]
26. Mendes-Felipe, C.; Veloso-Fernández, A.; Vilas-Vilela, J.L.; Ruiz-Rubio, L. Hybrid Organic–Inorganic Membranes for Photocatalytic Water Remediation. *Catalysts* **2022**, *12*, 180. [[CrossRef](#)]
27. Roy, S.; Singha, N.R. Polymeric nanocomposite membranes for next generation pervaporation process: Strategies, challenges and future prospects. *Membranes* **2017**, *7*, 53. [[CrossRef](#)]
28. Barbaros, I.; Yang, Y.; Safaei, B.; Yang, Z.; Qin, Z.; Asmael, M. State-of-the-art review of fabrication, application, and mechanical properties of functionally graded porous nanocomposite materials. *Nanotechnol. Rev.* **2022**, *11*, 321–371. [[CrossRef](#)]
29. Mohamed, A.; Yousef, S.; Tonkonogovas, A.; Makarevicius, V.; Stankevicius, A. High performance of PES-GNs MMMs for gas separation and selectivity. *Arab. J. Chem.* **2022**, *15*, 103565. [[CrossRef](#)]
30. Ghazi, F.M.G.; Abbaspour, M.; Rahimpour, M.R. Transport phenomena in gas membrane separations. In *Current Trends and Future Developments on (Bio-) Membranes*; Elsevier: Amsterdam, The Netherlands, 2022; pp. 193–208.
31. Saini, N.; Awasthi, K. Insights into the progress of polymeric nano-composite membranes for hydrogen separation and purification in the direction of sustainable energy resources. *Sep. Purif. Technol.* **2022**, *282*, 120029. [[CrossRef](#)]
32. Wang, C.; Park, M.J.; Yu, H.; Matsuyama, H.; Drioli, E.; Shon, H.K. Recent advances of nanocomposite membranes using layer-by-layer assembly. *J. Membr. Sci.* **2022**, *661*, 120926. [[CrossRef](#)]
33. Rath, R.; Kumar, P.; Rana, D.; Mishra, V.; Kumar, A.; Mohanty, S.; Nayak, S.K. Sulfonated PVDF nanocomposite membranes tailored with graphene oxide nanoparticles: Improved proton conductivity and membrane selectivity thereof. *J. Mater. Sci.* **2022**, *57*, 3565–3585. [[CrossRef](#)]
34. Patel, H.D.; Acharya, N.K. Transport, Spectroscopic, and Electrical Properties of Thermally Rearranged Nanocomposite Membranes. *Chem. Eng. Technol.* **2022**, *45*, 2223–2233. [[CrossRef](#)]
35. Ioniță, M.; Vlăsceanu, G.M.; Watzlawek, A.A.; Voicu, S.I.; Burns, J.S.; Iovu, H. Graphene and functionalized graphene: Extraordinary prospects for nanobiocomposite materials. *Compos. Part B Eng.* **2017**, *121*, 34–57. [[CrossRef](#)]
36. Song, P.; Wang, H. High-performance polymeric materials through hydrogen-bond cross-linking. *Adv. Mater.* **2020**, *32*, 1901244. [[CrossRef](#)]
37. Vatanpour, V.; Jouyandeh, M.; Akhi, H.; Khadem, S.S.M.; Ganjali, M.R.; Moradi, H.; Mirsadeghi, S.; Badii, A.; Esmaeili, A.; Rabiee, N. Hyperbranched polyethylenimine functionalized silica/polysulfone nanocomposite membranes for water purification. *Chemosphere* **2022**, *290*, 133363. [[CrossRef](#)]

38. Alavi, M.; Thomas, S.; Sreedharan, M. Modification of silica nanoparticles for antibacterial activities: Mechanism of action. *Micro Nano Bio Asp.* **2022**, *1*, 49–58.
39. Barzegar, T.; Hassanajili, S. Fabrication and characterization of dual layer PEBA<sub>X</sub>-SiO<sub>2</sub>/polyethersulfone nanocomposite membranes for separation of CO<sub>2</sub>/CH<sub>4</sub> gases. *J. Appl. Polym. Sci.* **2022**, *139*, 51624. [[CrossRef](#)]
40. Lakhotia, S.R.; Mukhopadhyay, M.; Kumari, P. Surface-modified nanocomposite membranes. *Sep. Purif. Rev.* **2018**, *47*, 288–305. [[CrossRef](#)]
41. Ahmadian-Alam, L.; Mahdavi, H. A novel polysulfone-based ternary nanocomposite membrane consisting of metal-organic framework and silica nanoparticles: As proton exchange membrane for polymer electrolyte fuel cells. *Renew. Energy* **2018**, *126*, 630–639. [[CrossRef](#)]
42. Khadry, N.H.; Abdelsalam, M.E. Polymer-silica nanocomposite membranes for CO<sub>2</sub> capturing. *Arab. J. Chem.* **2020**, *13*, 557–567. [[CrossRef](#)]
43. Yuan, H.; Liu, J.; Zhang, X.; Chen, L.; Zhang, Q.; Ma, L. Recent advances in membrane-based materials for desalination and gas separation. *J. Clean. Prod.* **2023**, *387*, 135845. [[CrossRef](#)]
44. Shanmugasundar, S.; Kannan, N.; Sundaravadivel, E.; Zsolt, S.; Mukunthan, K.; Manokaran, J.; Narendranath, J.; Kamalakannan, V.; Kavitha, P.; Prabhu, V. Study on the inflammatory response of PMMA/polystyrene/silica nanocomposite membranes for drug delivery and dental applications. *PLoS ONE* **2019**, *14*, e0209948. [[CrossRef](#)] [[PubMed](#)]
45. Liu, T.-Y.; Yuan, H.-G.; Liu, Y.-Y.; Ren, D.; Su, Y.-C.; Wang, X. Metal-organic framework nanocomposite thin films with interfacial bindings and self-standing robustness for high water flux and enhanced ion selectivity. *ACS Nano* **2018**, *12*, 9253–9265. [[CrossRef](#)] [[PubMed](#)]
46. Goncharenko, A.A.; Tarasyuk, I.A.; Marfin, Y.S.; Grzhegorzhevskii, K.V.; Muslimov, A.R.; Bondarenko, A.B.; Lebedev, M.D.; Kuz'min, I.A.; Vashurin, A.S.; Lepik, K.V. DDAO Controlled Synthesis of Organo-Modified Silica Nanoparticles with Encapsulated Fluorescent Boron Dipyrins and Study of Their Uptake by Cancerous Cells. *Molecules* **2020**, *25*, 3802. [[CrossRef](#)]
47. Hanif, M.; Shin, H.; Chun, D.; Kim, H.G.; Kwac, L.K.; Kim, Y.S. Photocatalytic VOCs Degradation Efficiency of Polypropylene Membranes by Incorporation of TiO<sub>2</sub> Nanoparticles. *Membranes* **2023**, *13*, 50. [[CrossRef](#)]
48. Shen, L.; Huang, Z.; Liu, Y.; Li, R.; Xu, Y.; Jakaj, G.; Lin, H. Polymeric membranes incorporated with ZnO nanoparticles for membrane fouling mitigation: A brief review. *Front. Chem.* **2020**, *8*, 224. [[CrossRef](#)]
49. Douna, I.; Farrukh, S.; Pervaiz, E.; Hussain, A.; Fan, X.F.; Salahuddin, Z. Blending of ZnO Nanorods in Cellulose Acetate Mixed Matrix Membrane for Enhancement of CO<sub>2</sub> Permeability. *J. Polym. Environ.* **2023**, 1–17. [[CrossRef](#)]
50. Yazid, A.F.; Mukhtar, H.; Nasir, R.; Mohshim, D.F. Incorporating Carbon Nanotubes in Nanocomposite Mixed-Matrix Membranes for Gas Separation: A Review. *Membranes* **2022**, *12*, 589. [[CrossRef](#)]
51. Lan, Q.; Yan, N.; Yang, H.; Wang, Y. Nanocomposite block copolymer membranes with enhanced permeance and robustness by carbon nanotube doping. *Compos. Commun.* **2022**, *29*, 101025. [[CrossRef](#)]
52. Gogoi, M.; Goswami, R.; Borah, A.; Hazarika, S. In situ Assembly of Functionalized Single-Walled Carbon Nanotube with partially reduced Graphene oxide Nanocomposite Membrane for Chiral Separation of  $\beta$ -substituted- $\alpha$ -amino acids. *Sep. Purif. Technol.* **2022**, *283*, 120201. [[CrossRef](#)]
53. Kausar, A. Polymeric nanocomposite with polyhedral oligomeric silsesquioxane and nanocarbon (fullerene, graphene, carbon nanotube, nanodiamond)—Futuristic headways. *Polym.-Plast. Technol. Mater.* **2023**, 1–14. [[CrossRef](#)]
54. Kausar, A. Poly (methyl methacrylate)/Fullerene nanocomposite—Factors and applications. *Polym.-Plast. Technol. Mater.* **2022**, *61*, 593–608. [[CrossRef](#)]
55. Mohammed, M.; Yahia, I. Towards multifunctional applications of Fullerene-filled (PVA-PEG) polymeric nanocomposite films: Structural, optical, and electrical properties. *Phys. Scr.* **2022**, *97*, 065813. [[CrossRef](#)]
56. Norouzi, A.; Lay, E.N.; Hosseinkhani, A.; Chapalaghi, M. Functionalized nanodiamonds in polyurethane mixed matrix membranes for carbon dioxide separation. *Results Mater.* **2022**, *13*, 100243. [[CrossRef](#)]
57. Ahmadijokani, F.; Molavi, H.; Bahi, A.; Wuttke, S.; Kamkar, M.; Rojas, O.J.; Ko, F.; Arjmand, M. Electrospun Nanofibers of Chitosan/Polyvinyl Alcohol/UiO-66/Nanodiamond: Versatile Adsorbents for Wastewater Remediation and Organic Dye Removal. *Chem. Eng. J.* **2022**, *457*, 141176. [[CrossRef](#)]
58. Pandey, K.; Dwivedi, M.M.; Sanjay, S.S. A brief review on synthesis and application of polymer-nanodiamond composite. *Mater. Today Proc.* **2022**, *68*, 2772–2780. [[CrossRef](#)]
59. Johnson, D.J.; Hilal, N. Nanocomposite nanofiltration membranes: State of play and recent advances. *Desalination* **2022**, *524*, 115480. [[CrossRef](#)]
60. Wu, J.; Chung, T.S. Supramolecular Polymer Network Membranes with Molecular-Sieving Nanocavities for Efficient Pre-Combustion CO<sub>2</sub> Capture. *Small Methods* **2022**, *6*, 2101288. [[CrossRef](#)]
61. de Sá, M.; Pinto, A.; Oliveira, V. Passive direct methanol fuel cells as a sustainable alternative to batteries in hearing aid devices—An overview. *Int. J. Hydrogen Energy* **2022**, *47*, 16552–16567. [[CrossRef](#)]
62. You, X.; Zhang, Q.; Yang, J.; Dong, S. Review on 3D-printed graphene-reinforced composites for structural applications. *Compos. Part A Appl. Sci. Manuf.* **2023**, *167*, 107420. [[CrossRef](#)]
63. Berger, C.; Song, Z.; Li, X.; Wu, X.; Brown, N.; Naud, C.; Mayou, D.; Li, T.; Hass, J.; Marchenkov, A.N. Electronic confinement and coherence in patterned epitaxial graphene. *Science* **2006**, *312*, 1191–1196. [[CrossRef](#)]

64. Hong, N.; Kireev, D.; Zhao, Q.; Chen, D.; Akinwande, D.; Li, W. Roll-to-Roll Dry Transfer of Large-Scale Graphene. *Adv. Mater.* **2022**, *34*, 2106615. [[CrossRef](#)]
65. Chen, X.; Fan, K.; Liu, Y.; Li, Y.; Liu, X.; Feng, W.; Wang, X. Recent advances in fluorinated graphene from synthesis to applications: Critical review on functional chemistry and structure engineering. *Adv. Mater.* **2022**, *34*, 2101665. [[CrossRef](#)]
66. Fadel, Y.; Thickett, S.C.; Agarwal, V.; Zetterlund, P.B. Synthesis of graphene-based polymeric nanocomposites using emulsion techniques. *Prog. Polym. Sci.* **2022**, *125*, 101476. [[CrossRef](#)]
67. Narayanam, P.K.; Botcha, V.D.; Ghosh, M.; Major, S.S. Growth and Photocatalytic Behaviour of Transparent Reduced GO-ZnO Nanocomposite Sheets. *Nanotechnology* **2019**, *30*, 485601. [[CrossRef](#)]
68. Zandiatashbar, A.; Lee, G.-H.; An, S.J.; Lee, S.; Mathew, N.; Terrones, M.; Hayashi, T.; Picu, C.R.; Hone, J.; Koratkar, N. Effect of defects on the intrinsic strength and stiffness of graphene. *Nat. Commun.* **2014**, *5*, 3186. [[CrossRef](#)] [[PubMed](#)]
69. Shen, X.J.; Zeng, X.L.; Dang, C.Y. Graphene Composites. *Handb. Graphene* **2019**, *1*, 1–25.
70. Zhou, Q.; Xia, G.; Du, M.; Lu, Y.; Xu, H. Scotch-tape-like exfoliation effect of graphene quantum dots for efficient preparation of graphene nanosheets in water. *Appl. Surf. Sci.* **2019**, *483*, 52–59. [[CrossRef](#)]
71. Lee, H.; Lee, K.S. Interlayer Distance Controlled Graphene, Supercapacitor and Method of Producing the Same. U.S. Patent 10,214,422, 26 February 2019.
72. Omran, B.; Baek, K.-H. Graphene-derived antibacterial nanocomposites for water disinfection: Current and future perspectives. *Environ. Pollut.* **2022**, *298*, 118836. [[CrossRef](#)] [[PubMed](#)]
73. Ding, J.; Zhao, H.; Yu, H. Bio-inspired Multifunctional Graphene-Epoxy Anticorrosion Coatings by Low-Defect Engineered Graphene. *ACS Nano* **2022**, *16*, 710–720. [[CrossRef](#)]
74. Zhang, M.; Shan, Y.; Kong, Q.; Pang, H. Applications of Metal-Organic Framework-Graphene Composite Materials in Electrochemical Energy Storage. *FlatChem* **2022**, *32*, 100332. [[CrossRef](#)]
75. Aiswaria, P.; Mohamed, S.N.; Singaravelu, D.L.; Brindhadevi, K.; Pugazhendhi, A. A review on graphene/graphene oxide supported electrodes for microbial fuel cell applications: Challenges and prospects. *Chemosphere* **2022**, *296*, 133983.
76. Panwar, N.; Soehartono, A.M.; Chan, K.K.; Zeng, S.; Xu, G.; Qu, J.; Coquet, P.; Yong, K.-T.; Chen, X. Nanocarbons for biology and medicine: Sensing, imaging, and drug delivery. *Chem. Rev.* **2019**, *119*, 9559–9656. [[CrossRef](#)] [[PubMed](#)]
77. Obraztsov, I.; Bakandritsos, A.; Šedajová, V.; Langer, R.; Jakubec, P.; Zoppellaro, G.; Pykal, M.; Presser, V.; Otyepka, M.; Zbořil, R. Graphene Acid for Lithium-Ion Batteries—Carboxylation Boosts Storage Capacity in Graphene. *Adv. Energy Mater.* **2022**, *12*, 2103010. [[CrossRef](#)]
78. Yang, Y.; Cheng, Y.; Yang, M.; Qian, G.; Peng, S.; Qi, F.; Shuai, C. Semicohherent strengthens graphene/zinc scaffolds. *Mater. Today Nano* **2022**, *17*, 100163. [[CrossRef](#)]
79. Grasseschi, D.; Silva, W.C.; de Souza Paiva, R.; Starke, L.D.; do Nascimento, A.S. Surface coordination chemistry of graphene: Understanding the coordination of single transition metal atoms. *Coord. Chem. Rev.* **2020**, *422*, 213469. [[CrossRef](#)]
80. Trache, D.; Tarchoun, A.F.; Abdelaziz, A.; Bessa, W.; Hussin, M.H.; Brosse, N.; Thakur, V.K. Cellulose nanofibrils-graphene hybrids: Recent advances in fabrication, properties, and applications. *Nanoscale* **2022**, *14*, 12515–12546. [[CrossRef](#)]
81. Nimbalkar, A.S.; Tiwari, S.K.; Ha, S.K.; Hong, C.K. An efficient water saving step during the production of graphene oxide via chemical exfoliation of graphite. *Mater. Today Proc.* **2020**, *21*, 1749–1754. [[CrossRef](#)]
82. Balaji, A.; Yang, S.; Wang, J.; Zhang, J. Graphene oxide-based nanostructured DNA sensor. *Biosensors* **2019**, *9*, 74. [[CrossRef](#)]
83. Halim, A.; Luo, Q.; Ju, Y.; Song, G. A mini review focused on the recent applications of graphene oxide in stem cell growth and differentiation. *Nanomaterials* **2018**, *8*, 736. [[CrossRef](#)] [[PubMed](#)]
84. Lin, L.; Peng, H.; Liu, Z. Synthesis challenges for graphene industry. *Nat. Mater.* **2019**, *18*, 520–524. [[CrossRef](#)] [[PubMed](#)]
85. Arvizu-Rodriguez, L.; Paramo-García, U.; Caballero-Briones, F. Low resistance, high mobility reduced graphene oxide films prepared with commercial antioxidant supplements. *Mater. Lett.* **2020**, *276*, 128176. [[CrossRef](#)]
86. Lin, T.-N.; Santiago, S.R.M.; Yuan, C.-T.; Chiu, K.-P.; Shen, J.-L.; Wang, T.-C.; Kuo, H.-C.; Chiu, C.-H.; Yao, Y.-C.; Lee, Y.-J. Enhanced performance of GaN-based ultraviolet light emitting diodes by photon recycling using graphene quantum dots. *Sci. Rep.* **2017**, *7*, 7108. [[CrossRef](#)]
87. Magne, T.M.; de Oliveira Vieira, T.; Alencar, L.M.R.; Junior, F.F.M.; Gemini-Piperni, S.; Carneiro, S.V.; Fehine, L.M.; Freire, R.M.; Golokhvast, K.; Metrangolo, P. Graphene and its derivatives: Understanding the main chemical and medicinal chemistry roles for biomedical applications. *J. Nanostructure Chem.* **2021**, *12*, 693–727. [[CrossRef](#)]
88. Deng, X.; Zou, C.; Han, Y.; Lin, L.-C.; Ho, W.W. Computational Evaluation of Carriers in Facilitated Transport Membranes for Postcombustion Carbon Capture. *J. Phys. Chem. C* **2020**, *124*, 46. [[CrossRef](#)]
89. Szomek, M.; Moesgaard, L.; Reinholdt, P.; Hald, S.B.H.; Petersen, D.; Krishnan, K.; Covey, D.F.; Kongsted, J.; Wüstner, D. Membrane organization and intracellular transport of a fluorescent analogue of 27-hydroxycholesterol. *Chem. Phys. Lipids* **2020**, *233*, 105004. [[CrossRef](#)]
90. Lee, J.; Aluru, N.R. Water-solubility-driven separation of gases using graphene membrane. *J. Membr. Sci.* **2013**, *428*, 546–553. [[CrossRef](#)]
91. Liu, N.; Cheng, J.; Hou, W.; Yang, X.; Zhou, J. Unsaturated Zn-N<sub>2</sub>-O active sites derived from hydroxyl in graphene oxide and zinc atoms in core shell ZIF-8@ZIF-67 nanocomposites enhanced CO<sub>2</sub> adsorption capacity. *Microporous Mesoporous Mater.* **2020**, *312*, 110786. [[CrossRef](#)]



92. Miricioiu, M.G.; Iacob, C.; Nechifor, G.; Niculescu, V.-C. High selective mixed membranes based on mesoporous MCM-41 and MCM-41-NH<sub>2</sub> particles in a polysulfone matrix. *Front. Chem.* **2019**, *7*, 332. [[CrossRef](#)]
93. Rezakazemi, M.; Sadrzadeh, M.; Matsuura, T. Thermally stable polymers for advanced high-performance gas separation membranes. *Prog. Energy Combust. Sci.* **2018**, *66*, 1–41. [[CrossRef](#)]
94. Koenig, S.P.; Wang, L.; Pellegrino, J.; Bunch, J.S. Selective molecular sieving through porous graphene. *Nat. Nanotechnol.* **2012**, *7*, 728–732. [[CrossRef](#)] [[PubMed](#)]
95. Du, Y.C.; Huang, L.J.; Wang, Y.X.; Yang, K.; Tang, J.G.; Wang, Y.; Cheng, M.M.; Zhang, Y.; Kipper, M.J.; Belfiore, L.A. Recent developments in graphene-based polymer composite membranes: Preparation, mass transfer mechanism, and applications. *J. Appl. Polym. Sci.* **2019**, *136*, 47761. [[CrossRef](#)]
96. Li, H.; Song, Z.; Zhang, X.; Huang, Y.; Li, S.; Mao, Y.; Ploehn, H.J.; Bao, Y.; Yu, M. Ultrathin, molecular-sieving graphene oxide membranes for selective hydrogen separation. *Science* **2013**, *342*, 95–98. [[CrossRef](#)]
97. Dong, G.; Hou, J.; Wang, J.; Zhang, Y.; Chen, V.; Liu, J. Enhanced CO<sub>2</sub>/N<sub>2</sub> separation by porous reduced graphene oxide/Pebax mixed matrix membranes. *J. Membr. Sci.* **2016**, *520*, 860–868. [[CrossRef](#)]
98. Ibrahim, A.F.; Banihashemi, F.; Lin, Y. Graphene oxide membranes with narrow inter-sheet galleries for enhanced hydrogen separation. *Chem. Commun.* **2019**, *55*, 3077–3080. [[CrossRef](#)] [[PubMed](#)]
99. Yang, Y.H.; Bolling, L.; Priolo, M.A.; Grunlan, J.C. Super gas barrier and selectivity of graphene oxide-polymer multilayer thin films. *Adv. Mater.* **2013**, *25*, 503–508. [[CrossRef](#)]
100. Vinodh, R.; Atchudan, R.; Kim, H.-J.; Yi, M. Recent advancements in polysulfone based membranes for fuel cell (PEMFCs, DMFCs and AMFCs) applications: A critical review. *Polymers* **2022**, *14*, 300. [[CrossRef](#)] [[PubMed](#)]
101. Ali, M.E.; Shahat, A.; Ayoub, T.I.; Kamel, R.M. Fabrication of high flux polysulfone/mesoporous silica nanocomposite ultrafiltration membranes for industrial wastewater treatment. *Biointerface Res. Appl. Chem.* **2022**, *12*, 7556–7572.
102. Sherugar, P.; Déon, S.; Nagaraja, K.; Padaki, M. Tailoring the structure of polysulfone nanocomposite membranes by incorporating iron oxide doped aluminium oxide for excellent separation performance and antifouling property. *Environ. Sci. Water Res. Technol.* **2022**, *8*, 1059–1077. [[CrossRef](#)]
103. Costa Flores, M.; Figueiredo, K.C.d.S. Asymmetric oxygen-functionalized carbon nanotubes dispersed in polysulfone for CO<sub>2</sub> separation. *J. Appl. Polym. Sci.* **2023**, *140*, e53303. [[CrossRef](#)]
104. Said, N.; Mansur, S.; Zainol Abidin, M.N.; Ismail, A.F. Fabrication and characterization of polysulfone/iron oxide nanoparticle mixed matrix hollow fiber membranes for hemodialysis: Effect of dope extrusion rate and air gap. *J. Membr. Sci. Res.* **2023**, *9*, 1972553.
105. Zahri, K.; Goh, P.; Ismail, A. The incorporation of graphene oxide into polysulfone mixed matrix membrane for CO<sub>2</sub>/CH<sub>4</sub> separation. In *IOP Conference Series: Earth and Environmental Science*; IOP Publishing: Bristol, UK, 2016; p. 012007.
106. Zahri, K.; Wong, K.; Goh, P.; Ismail, A. Graphene oxide/polysulfone hollow fiber mixed matrix membranes for gas separation. *RSC Adv.* **2016**, *6*, 89130–89139. [[CrossRef](#)]
107. Sainath, K.; Modi, A.; Bellare, J. In-situ growth of zeolitic imidazolate framework-67 nanoparticles on polysulfone/graphene oxide hollow fiber membranes enhance CO<sub>2</sub>/CH<sub>4</sub> separation. *J. Membr. Sci.* **2020**, *614*, 118506. [[CrossRef](#)]
108. Zhu, X.; Zhou, Y.; Hao, J.; Bao, B.; Bian, X.; Jiang, X.; Pang, J.; Zhang, H.; Jiang, Z.; Jiang, L. A charge-density-tunable three/two-dimensional polymer/graphene oxide heterogeneous nanoporous membrane for ion transport. *ACS Nano* **2017**, *11*, 10816–10824. [[CrossRef](#)] [[PubMed](#)]
109. Liu, J.; Pan, Y.; Xu, J.; Wang, Z.; Zhu, H.; Liu, G.; Zhong, J.; Jin, W. Introducing amphiphatic copolymer into intermediate layer to fabricate ultra-thin Pebax composite membrane for efficient CO<sub>2</sub> capture. *J. Membr. Sci.* **2023**, *667*, 121183. [[CrossRef](#)]
110. Hieu, N.H.; Phat, N.T.; Giang, N.T.H.; Tinh, N.T.; Dat, N.M.; Phong, M.T. Recovery of furfural by pervaporation technology using the ceramic tubular supported graphene-polydimethylsiloxane nanocomposite membranes. *FlatChem* **2022**, *34*, 100402. [[CrossRef](#)]
111. Yang, J.; Chen, A.; Liu, F.; Gu, L.; Xie, X.; Ding, Z. Hybrid coating of polydimethylsiloxane with nano-ZrO<sub>2</sub> on magnesium alloy for superior corrosion resistance. *Ceram. Int.* **2022**, *48*, 35280–35289. [[CrossRef](#)]
112. Zhang, W.; Shi, Y.; Wang, B.; Han, Y.; Zhang, R. High-strength electrospun polydimethylsiloxane/polytetrafluoroethylene hybrid membranes with stable and controllable coral-like structures. *Compos. Part A Appl. Sci. Manuf.* **2023**, *164*, 107316. [[CrossRef](#)]
113. Berean, K.J.; Ou, J.Z.; Nour, M.; Field, M.R.; Alsaif, M.M.; Wang, Y.; Ramanathan, R.; Bansal, V.; Kentish, S.; Doherty, C.M. Enhanced gas permeation through graphene nanocomposites. *J. Phys. Chem. C* **2015**, *119*, 13700–13712. [[CrossRef](#)]
114. Koolivand, H.; Sharif, A.; Chehrizi, E.; Kashani, M.R.; Paran, S.M.R. Mixed-matrix membranes comprising graphene-oxide nanosheets for CO<sub>2</sub>/CH<sub>4</sub> separation: A comparison between glassy and rubbery polymer matrices. *Polym. Sci. Ser. A* **2016**, *58*, 801–809. [[CrossRef](#)]
115. Zhang, Q.; Yang, Y.; Fan, H.; Feng, L.; Wen, G.; Qin, L.-C. Synthesis of graphene oxide using boric acid in hummers method. *Colloids Surf. A Physicochem. Eng. Asp.* **2022**, *652*, 129802. [[CrossRef](#)]
116. Ha, H.; Park, J.; Ando, S.; Kim, C.B.; Nagai, K.; Freeman, B.D.; Ellison, C.J. Gas permeation and selectivity of poly (dimethylsiloxane)/graphene oxide composite elastomer membranes. *J. Membr. Sci.* **2016**, *518*, 131–140. [[CrossRef](#)]
117. Tumnantong, D.; Srisamrid, K.; Poompradub, S.; Prasassarakich, P. Preparation of poly (methyl methacrylate)-silica nanocomposites via DMP-assisted RAFT polymerization and NR/PMMA-RAFT-SiO<sub>2</sub> hybrid membrane for pervaporation. *Eur. Polym. J.* **2022**, *168*, 111088. [[CrossRef](#)]

118. Zakaria, N.; Zaliman, S.; Leo, C.; Ahmad, A.; Ooi, B.; Poh, P.E. Electrochemical cleaning of superhydrophobic polyvinylidene fluoride/polymethyl methacrylate/carbon black membrane after membrane distillation. *J. Taiwan Inst. Chem. Eng.* **2022**, *138*, 104448. [[CrossRef](#)]
119. Mohammed, M.; Khafagy, R.; Hussien, M.S.; Sakr, G.; Ibrahim, M.A.; Yahia, I.; Zahran, H. Enhancing the structural, optical, electrical, properties and photocatalytic applications of ZnO/PMMA nanocomposite membranes: Towards multifunctional membranes. *J. Mater. Sci. Mater. Electron.* **2022**, *33*, 1977–2002. [[CrossRef](#)]
120. Baldanza, A.; Pastore Carbone, M.G.; Brondi, C.; Manikas, A.C.; Mensitieri, G.; Pavlou, C.; Scherillo, G.; Galiotis, C. Chemical Vapour Deposition Graphene–PMMA Nanolaminates for Flexible Gas Barrier. *Membranes* **2022**, *12*, 611. [[CrossRef](#)]
121. Pavlou, C.; Pastore Carbone, M.G.; Manikas, A.C.; Trakakis, G.; Koral, C.; Papari, G.; Andreone, A.; Galiotis, C. Effective EMI shielding behaviour of thin graphene/PMMA nanolaminates in the THz range. *Nat. Commun.* **2021**, *12*, 4655. [[CrossRef](#)] [[PubMed](#)]
122. Agrawal, K.V.; Benck, J.D.; Yuan, Z.; Misra, R.P.; Govind Rajan, A.; Eatmon, Y.; Kale, S.; Chu, X.S.; Li, D.O.; Gong, C. Fabrication, pressure testing, and nanopore formation of single-layer graphene membranes. *J. Phys. Chem. C* **2017**, *121*, 14312–14321. [[CrossRef](#)]
123. Jin, J.; Zhu, S.; Wang, Z.; Bi, X.; Shi, Y.; Shi, Y.; Zhang, Y. *Thin Film of Polyimide/Mof Nanocomposite Membrane with Substantially Improved Stability for CO<sub>2</sub>/CH<sub>4</sub> Separation*; Social Science Research Network; Elsevier: Amsterdam, The Netherlands, 2022; pp. 1–30.
124. Muhammad, S.; Niazi, J.H.; Shawuti, S.; Qureshi, A. Functional POSS based polyimide nanocomposite for enhanced structural, thermal, antifouling and antibacterial properties. *Mater. Today Commun.* **2022**, *31*, 103287. [[CrossRef](#)]
125. Zhu, S.; Bi, X.; Shi, Y.; Shi, Y.; Zhang, Y.; Jin, J.; Wang, Z. Thin Films Based on Polyimide/Metal–Organic Framework Nanoparticle Composite Membranes with Substantially Improved Stability for CO<sub>2</sub>/CH<sub>4</sub> Separation. *ACS Appl. Nano Mater.* **2022**, *5*, 8997–9007. [[CrossRef](#)]
126. Melicchio, A.; Favvas, E.P. Preparation and characterization of graphene oxide as a candidate filler material for the preparation of mixed matrix polyimide membranes. *Surf. Coat. Technol.* **2018**, *349*, 1058–1068. [[CrossRef](#)]
127. Shishatskiy, S.; Makrushin, V.; Levin, I.; Merten, P.; Matson, S.; Khotimskiy, V. Effect of Immobilization of Phenolic Antioxidant on Thermo-Oxidative Stability and Aging of Poly (1-trimethylsilyl-1-propyne) in View of Membrane Application. *Polymers* **2022**, *14*, 462. [[CrossRef](#)]
128. Golubev, G.; Sokolov, S.; Rokhmanka, T.; Makaev, S.; Borisov, I.; Khashirova, S.; Volkov, A. High Efficiency Membranes Based on PTMSP and Hyper-Crosslinked Polystyrene for Toxic Volatile Compounds Removal from Wastewater. *Polymers* **2022**, *14*, 2944. [[CrossRef](#)] [[PubMed](#)]
129. Kalmykov, D.; Balyinin, A.; Yushkin, A.; Grushevenko, E.; Sokolov, S.; Malakhov, A.; Volkov, A.; Bazhenov, S. Membranes Based on PTMSP/PVTMS Blends for Membrane Contactor Applications. *Membranes* **2022**, *12*, 1160. [[CrossRef](#)] [[PubMed](#)]
130. Olivieri, L.; Ligi, S.; De Angelis, M.G.; Cucca, G.; Pettinau, A. Effect of graphene and graphene oxide nanoplatelets on the gas permselectivity and aging behavior of poly (trimethylsilyl propyne)(PTMSP). *Ind. Eng. Chem. Res.* **2015**, *54*, 11199–11211. [[CrossRef](#)]
131. Alberto, M.; Bhavsar, R.; Luque-Alled, J.M.; Vijayaraghavan, A.; Budd, P.M.; Gorgojo, P. Impeded physical aging in PIM-1 membranes containing graphene-like fillers. *J. Membr. Sci.* **2018**, *563*, 513–520. [[CrossRef](#)]
132. Zhang, D.; Xu, S.; Wan, R.; Yang, Y.; He, R. Functionalized graphene oxide cross-linked poly (2, 6-dimethyl-1, 4-phenylene oxide)-based anion exchange membranes with superior ionic conductivity. *J. Power Sources* **2022**, *517*, 230720. [[CrossRef](#)]
133. Chen, J.; Zhang, M.; Shen, C.; Gao, S. Preparation and Characterization of Non-N-Bonded Side-Chain Anion Exchange Membranes Based on Poly (2, 6-dimethyl-1, 4-phenylene oxide). *Ind. Eng. Chem. Res.* **2022**, *61*, 1715–1724. [[CrossRef](#)]
134. Chu, X.; Miao, S.; Zhou, A.; Liu, S.; Liu, L.; Li, N. A strategy to design quaternized poly (2, 6-dimethyl-1, 4-phenylene oxide) anion exchange membranes by atom transfer radical coupling. *J. Membr. Sci.* **2022**, *649*, 120397. [[CrossRef](#)]
135. Rea, R.; Ligi, S.; Christian, M.; Morandi, V.; Giacinti Baschetti, M.; De Angelis, M.G. Permeability and selectivity of PPO/graphene composites as mixed matrix membranes for CO<sub>2</sub> capture and gas separation. *Polymers* **2018**, *10*, 129. [[CrossRef](#)] [[PubMed](#)]
136. Theravalappil, R.; Rahaman, M. Patents on graphene-based polymer composites and their applications. In *Polymer Nanocomposites Containing Graphene*; Elsevier: Amsterdam, The Netherlands, 2022; pp. 615–638.
137. Ren, F.; Tan, W.; Duan, Q.; Jin, Y.; Pei, L.; Ren, P.; Yan, D. Ultra-low gas permeable cellulose nanofiber nanocomposite films filled with highly oriented graphene oxide nanosheets induced by shear field. *Carbohydr. Polym.* **2019**, *209*, 310–319. [[CrossRef](#)]
138. Rather, A.H.; Khan, R.S.; Wani, T.U.; Beigh, M.A.; Sheikh, F.A. Overview on immobilization of enzymes on synthetic polymeric nanofibers fabricated by electrospinning. *Biotechnol. Bioeng.* **2022**, *119*, 9–33. [[CrossRef](#)]
139. Han, Y.; Xu, Y.; Zhang, S.; Li, T.; Ramakrishna, S.; Liu, Y. Progress of improving mechanical strength of electrospun nanofibrous membranes. *Macromol. Mater. Eng.* **2020**, *305*, 2000230. [[CrossRef](#)]
140. Peng, K.; Huang, H. Investigating the origin of the core-shell structure of polymeric nanofibers during fabrication process at the atomistic scale. *Appl. Surf. Sci.* **2023**, *608*, 155105. [[CrossRef](#)]
141. Nayl, A.A.; Abd-Elhamid, A.I.; Awwad, N.S.; Abdelgawad, M.A.; Wu, J.; Mo, X.; Gomha, S.M.; Aly, A.A.; Bräse, S. Review of the Recent Advances in Electrospun Nanofibers Applications in Water Purification. *Polymers* **2022**, *14*, 1594. [[CrossRef](#)] [[PubMed](#)]
142. Jiang, W.; Du, Y.; Ji, Y.; Zhou, Y.; Zhao, P.; Yu, D.G. Modernization of traditional Chinese condiments via electrospun polymeric nanocomposites. *ES Food Agrofor.* **2022**, *8*, 47–56. [[CrossRef](#)]



143. Mora-Boza, A.; López-Ruiz, E.; López-Donaire, M.L.; Jiménez, G.; Aguilar, M.R.; Marchal, J.A.; Pedraz, J.L.; Vázquez-Lasa, B.; Román, J.S.; Gálvez-Martín, P. Evaluation of Glycerylphosphate Crosslinked Semi-and Interpenetrated Polymer Membranes of Hyaluronic Acid and Chitosan for Tissue Engineering. *Polymers* **2020**, *12*, 2661. [[CrossRef](#)]
144. Morales-Zamudio, L.; Lozano, T.; Caballero-Briones, F.; Zamudio, M.A.; Angeles-San Martin, M.E.; de Lira-Gomez, P.; Martinez-Colunga, G.; Rodriguez-Gonzalez, F.; Neira, G.; Sanchez-Valdes, S. Structure and Mechanical Properties of Graphene Oxide-Reinforced Polycarbonate. *Mater. Chem. Phys.* **2020**, *261*, 124180. [[CrossRef](#)]
145. Lee, S.J.; Yoon, S.J.; Jeon, I.-Y. Graphene/Polymer Nanocomposites: Preparation, Mechanical Properties, and Application. *Polymers* **2022**, *14*, 4733. [[CrossRef](#)]
146. Kanjwal, M.A.; Ghaferi, A.A. Graphene Incorporated Electrospun Nanofiber for Electrochemical Sensing and Biomedical Applications: A Critical Review. *Sensors* **2022**, *22*, 8661. [[CrossRef](#)]
147. Jeong, K.; Kim, D.H.; Chung, Y.S.; Hwang, S.K.; Hwang, H.Y.; Kim, S.S. Effect of processing parameters of the continuous wet spinning system on the crystal phase of PVDF fibers. *J. Appl. Polym. Sci.* **2018**, *135*, 45712. [[CrossRef](#)]
148. Ganguly, S. Preparation/processing of polymer-graphene composites by different techniques. In *Polymer Nanocomposites Containing Graphene*; Elsevier: Amsterdam, The Netherlands, 2022; pp. 45–74.
149. Orasugh, J.T.; Ray, S.S. Graphene-Based Electrospun Fibrous Materials with Enhanced EMI Shielding: Recent Developments and Future Perspectives. *ACS Omega* **2022**, *7*, 33699–33718. [[CrossRef](#)]
150. Medeiros, G.B.; Lima, F.d.A.; de Almeida, D.S.; Guerra, V.G.; Aguiar, M.L. Modification and Functionalization of Fibers Formed by Electrospinning: A Review. *Membranes* **2022**, *12*, 861. [[CrossRef](#)]
151. Kausar, A.; Bocchetta, P. Polymer/graphene nanocomposite membranes: Status and emerging prospects. *J. Compos. Sci.* **2022**, *6*, 76. [[CrossRef](#)]
152. Kausar, A. Reinforced polyaniline nanocomposite nanofibers: Cutting-edge potential. *Polym.-Plast. Technol. Mater.* **2022**, *61*, 1–14. [[CrossRef](#)]
153. Widakdo, J.; Huang, T.-J.; Subrahmanya, T.; Austria, H.F.M.; Chou, H.-L.; Hung, W.-S.; Wang, C.-F.; Hu, C.-C.; Lee, K.-R.; Lai, J.-Y. Bioinspired ionic liquid-graphene based smart membranes with electrical tunable channels for gas separation. *Appl. Mater. Today* **2022**, *27*, 101441. [[CrossRef](#)]
154. Cooley, J.F. Improved methods of and apparatus for electrically separating the relatively volatile liquid component from the component of relatively fixed substances of composite fluids. *U. K. Pat.* **1900**, 6385, 19.
155. Yoo, B.M.; Shin, H.J.; Yoon, H.W.; Park, H.B. Graphene and graphene oxide and their uses in barrier polymers. *J. Appl. Polym. Sci.* **2014**, *131*, 39628. [[CrossRef](#)]
156. Novoselov, K.S.; Geim, A.K.; Morozov, S.V.; Jiang, D.-E.; Zhang, Y.; Dubonos, S.V.; Grigorieva, I.V.; Firsov, A.A. Electric field effect in atomically thin carbon films. *Science* **2004**, *306*, 666–669. [[CrossRef](#)]
157. Cai, D.; Song, M. Recent advance in functionalized graphene/polymer nanocomposites. *J. Mater. Chem.* **2010**, *20*, 7906–7915. [[CrossRef](#)]
158. Wang, Y.; Yang, G.; Wang, W.; Zhu, S.; Guo, L.; Zhang, Z.; Li, P. Effects of different functional groups in graphene nanofiber on the mechanical property of polyvinyl alcohol composites by the molecular dynamic simulations. *J. Mol. Liq.* **2019**, *277*, 261–268. [[CrossRef](#)]
159. Xin, Q.; Li, Z.; Li, C.; Wang, S.; Jiang, Z.; Wu, H.; Zhang, Y.; Yang, J.; Cao, X. Enhancing the CO<sub>2</sub> separation performance of composite membranes by the incorporation of amino acid-functionalized graphene oxide. *J. Mater. Chem. A* **2015**, *3*, 6629–6641. [[CrossRef](#)]
160. Quan, S.; Li, S.W.; Xiao, Y.C.; Shao, L. CO<sub>2</sub>-selective mixed matrix membranes (MMMs) containing graphene oxide (GO) for enhancing sustainable CO<sub>2</sub> capture. *Int. J. Greenh. Gas Control* **2017**, *56*, 22–29. [[CrossRef](#)]
161. Li, X.; Cheng, Y.; Zhang, H.; Wang, S.; Jiang, Z.; Guo, R.; Wu, H. Efficient CO<sub>2</sub> capture by functionalized graphene oxide nanosheets as fillers to fabricate multi-permselective mixed matrix membranes. *ACS Appl. Mater. Interfaces* **2015**, *7*, 5528–5537. [[CrossRef](#)] [[PubMed](#)]
162. Wang, S.; Liu, Y.; Huang, S.; Wu, H.; Li, Y.; Tian, Z.; Jiang, Z. Pebax-PEG-MWCNT hybrid membranes with enhanced CO<sub>2</sub> capture properties. *J. Membr. Sci.* **2014**, *460*, 62–70. [[CrossRef](#)]
163. Ge, L.; Zhu, Z.; Li, F.; Liu, S.; Wang, L.; Tang, X.; Rudolph, V. Investigation of Gas permeability in carbon nanotube (CNT)-polymer matrix membranes via modifying CNTs with functional groups/metals and controlling modification location. *J. Phys. Chem. C* **2011**, *115*, 6661–6670. [[CrossRef](#)]
164. Kim, S.; Chen, L.; Johnson, J.K.; Marand, E. Polysulfone and functionalized carbon nanotube mixed matrix membranes for gas separation: Theory and experiment. *J. Membr. Sci.* **2007**, *294*, 147–158. [[CrossRef](#)]
165. Liang, C.-Y.; Uchytíl, P.; Petrychkovych, R.; Lai, Y.-C.; Friess, K.; Sipek, M.; Reddy, M.M.; Suen, S.-Y. A comparison on gas separation between PES (polyethersulfone)/MMT (Na-montmorillonite) and PES/TiO<sub>2</sub> mixed matrix membranes. *Sep. Purif. Technol.* **2012**, *92*, 57–63. [[CrossRef](#)]
166. Momeni, S.; Pakizeh, M. Preparation, characterization and gas permeation study of PSf/MgO nanocomposite membrane. *Braz. J. Chem. Eng.* **2013**, *30*, 589–597.
167. Chen, X.Y.; Razzaz, Z.; Kaliaguine, S.; Rodrigue, D. Mixed matrix membranes based on silica nanoparticles and microcellular polymers for CO<sub>2</sub>/CH<sub>4</sub> separation. *J. Cell. Plast.* **2018**, *54*, 309–331. [[CrossRef](#)]

168. Karki, S.; Gohain, M.B.; Yadav, D.; Ingole, P.G. Nanocomposite and bio-nanocomposite polymeric materials/membranes development in energy and medical sector: A review. *Int. J. Biol. Macromol.* **2021**, *193*, 2121–2139. [[CrossRef](#)] [[PubMed](#)]
169. Pires, J.; Paula, C.D.d.; Souza, V.G.L.; Fernando, A.L.; Coelho, I. Understanding the barrier and mechanical behavior of different nanofillers in chitosan films for food packaging. *Polymers* **2021**, *13*, 721. [[CrossRef](#)] [[PubMed](#)]
170. Iravani, S. Nanomaterials and nanotechnology for water treatment: Recent advances. *Inorg. Nano-Met. Chem.* **2021**, *51*, 1615–1645. [[CrossRef](#)]
171. Jhaveri, J.H.; Murthy, Z. A comprehensive review on anti-fouling nanocomposite membranes for pressure driven membrane separation processes. *Desalination* **2016**, *379*, 137–154. [[CrossRef](#)]
172. Junaidi, N.F.D.; Othman, N.H.; Shahrudin, M.Z.; Alias, N.H.; Lau, W.J.; Ismail, A.F. Effect of graphene oxide (GO) and polyvinylpyrrolidone (PVP) additives on the hydrophilicity of composite polyethersulfone (PES) membrane. *Malays. J. Fundam. Appl. Sci.* **2019**, *15*, 361–366. [[CrossRef](#)]
173. Mahdavi Far, R.; Van der Bruggen, B.; Verliefde, A.; Cornelissen, E. A review of zeolite materials used in membranes for water purification: History, applications, challenges and future trends. *J. Chem. Technol. Biotechnol.* **2021**, *97*, 575–596. [[CrossRef](#)]

**Disclaimer/Publisher's Note:** The statements, opinions and data contained in all publications are solely those of the individual author(s) and contributor(s) and not of MDPI and/or the editor(s). MDPI and/or the editor(s) disclaim responsibility for any injury to people or property resulting from any ideas, methods, instructions or products referred to in the content.